UCRL-17899
cy. 2

University of California

Ernest O. Lawrence Radiation Laboratory

PHASE CONTOURS OF SCATTERING AMPLITUDES I
PHASE CONTOURS, ZEROS AND HIGH ENERGY BEHAVIOR

Charles B. Chiu, Richard J. Eden, and Chung-I Tan

October 30, 1967

RECEIVED
LAWRENCE
RADIATION LABORATORY

TWO-WEEK LOAN COPY

This is a Library Circulating Copy which may be borrowed for two weeks. For a personal retention copy, call Tech. Info. Division, Ext. 5545

UCRL-17899
cy. 2

DISCLAIMER

This document was prepared as an account of work sponsored by the United States Government. While this document is believed to contain correct information, neither the United States Government nor any agency thereof, nor the Regents of the University of California, nor any of their employees, makes any warranty, express or implied, or assumes any legal responsibility for the accuracy, completeness, or usefulness of any information, apparatus, product, or process disclosed, or represents that its use would not infringe privately owned rights. Reference herein to any specific commercial product, process, or service by its trade name, trademark, manufacturer, or otherwise, does not necessarily constitute or imply its endorsement, recommendation, or favoring by the United States Government or any agency thereof, or the Regents of the University of California. The views and opinions of authors expressed herein do not necessarily state or reflect those of the United States Government or any agency thereof or the Regents of the University of California.

Submitted to Physical Review

UCRL-17899
Preprint

UNIVERSITY OF CALIFORNIA
Lawrence Radiation Laboratory
Berkeley, California

AEC Contract No. W-7405-eng-48

PHASE CONTOURS OF SCATTERING AMPLITUDES I
PHASE CONTOURS, ZEROS AND HIGH ENERGY BEHAVIOR

Charles B. Chiu, Richard J. Eden, and Chung-I Tan

October 30, 1967

PHASE CONTOURS OF SCATTERING AMPLITUDES I: PHASE CONTOURS, ZEROS AND HIGH ENERGY BEHAVIOR*

Charles B. Chiu

CERN, Geneva, Switzerland

Richard J. Eden† and Chung-I Tan

Lawrence Radiation Laboratory
University of California
Berkeley, California

October 30, 1967

ABSTRACT

We define phase contours as curves along which the phase of an invariant scattering amplitude is a constant. These curves are sections of a complex surface, which we take either in the real (s,t) plane or in the complex plane of one of the variables. The relation between phase contours, zeros of the amplitude and high energy behavior is discussed. Characteristic features of phase contours are investigated in a variety of special models, and it is seen that basic assumptions about high energy behavior can readily be expressed in terms of the topology of the phase contours. Specific illustrations of phase contours are given for pion nucleon scattering based on phase shift-solutions at low and medium energies and on an extrapolation from Regge solutions at high energies.

1. INTRODUCTION

Our aim in this and subsequent papers is to explore the properties of scattering amplitudes, and other two body collision amplitudes, by means of a general study of their phases. Our first objective is to obtain the characteristic features of phase contours by studying special models. A phase contour is defined as the curve, or more generally the complex surface, on which the phase of an invariant amplitude takes a given constant (real) value. Their particular importance lies partly in the fact that phase contours contain enough information to specify an amplitude to within a real constant factor. However, our main motivation in developing their properties is that phase contours are rather simply related to high energy behavior, and they have striking features that are related to resonances and zeros of scattering amplitudes.

We wish to emphasize that this investigation, in the first instance, is exploratory and heuristic, rather than rigorous or deductive. In order to develop an intuition based on phase contours, it is first necessary to obtain their characteristics in many simple but important situations. In practice we will find it useful to study phase contours that are sections of a complex surface of constant phase taken (a) in the real s, real t plane, and (b) for complex s, and real t. In this paper we will be concerned mainly with phases of two body scattering amplitudes.

The experimental and theoretical importance of the phase of a scattering amplitude is well known for a variety of special values of

the invariant energy and momentum transfer variables. For example, in the physical region the phases of invariant amplitudes are closely related to polarization experiments and to other interference phenomena. The phase is also of great importance in near-forward scattering, since it is (almost) directly measurable experimentally and it is closely related to dispersion relations and the asymptotic behavior of scattering amplitudes. At medium and low energies the phase of an invariant amplitude will be influenced, sometimes strongly, by the rapid phase change of a partial wave amplitude near a resonance.

General methods for relating the asymptotic behavior of the phase of an amplitude to the asymptotic modulus of the amplitude have been summarized in a book by one of us.[1] The papers giving these relations are primarily concerned with rigorous rather than heuristic developments. However, they provide our initial motivation and will be essential in any rigorous study of phases, so some of ther results are briefly quoted in Section 2 of this paper.

The main reason that we put forward for the general study of phases is that it provides a new way of looking at the properties of scattering amplitudes. Phase contours, in particular, provide a graphic description of these properties that is remarkably simple in some circumstances. The problems to which we believe phase contours can be applied include:

(1) The development and comparison of phase shift solutions for scattering amplitudes. A phase contour diagram provides a convenient

picture of the complete solution for an invariant amplitude in the physical region, and permits the identification of such features as zeros of the amplitude at real values of energy and momentum transfer. It also indicates the regions where the solution for the amplitude is so complicated that further experiments would seem to be desirable.

(2) The comparison of scattering amplitudes that are obtained from specific asymptotic assumptions, for example within the framework of Regge theory. These assumptions could be generalized by replacing them with statements about the asymptotic characteristics of phase contours.

(3) The study of consistency conditions on scattering amplitudes related to high energy behavior, poles, and zeros, using crossing symmetry.

(4) The development of phenomenological solutions that relate both to high energy data, and to medium energy data in the resonance regions.

The above topics are preliminary problems related to much deeper questions to which one might hope also to apply the methods of phase contours. These include such questions as the possible connection between the low energy and high energy behavior in one channel, that is indicated by work on finite energy sum rules by Dolen, Horn, and Schmid.[2] It may also help towards understanding how to combine Regge behavior with resonance behavior in a consistent manner, although it is clear that there are formidable difficulties in this problem, as noted, for example, by Stirling and Chiu.[3]

In Section 2 we summarize theorems that relate to the phase of an amplitude, and indicate intuitive features of these theorems

which are later found useful in studying phase contours. In Section 3 we study phase contours for a pure Regge background, assuming that any resonances are too weak to affect the basic topology for real values of s and t. The relations between these phase contours and the Herglotz conditions are considered in Section 6, where we indicate the effects of zeros of amplitudes as well as the effects of phase oscillations. In Section 5 we consider interference effects that arise from resonances and background contributions, and again we consider the relation of consequent zeros and oscillations to asymptotic behavior. Similar questions are discussed for Reggeised resonance terms in Section 6. Some results of experimental studies of the phases of invariant amplitudes for pion nucleon scattering are given in Section 7. We obtain phase contours for these amplitudes from the phase shift solutions of scattering experiments up to about 1.5 GeV pion energy. They provide a convenient method for comparing different phase shift solutions, and for indicating where the amplitude is so complicated as to require more detailed experiments to confirm the validity of the solutions. In Section 8 we derive phase contours for pion nucleon invariant amplitudes that are based on an extrapolation from the Regge solutions to high energy scattering. Finally in Section 9 we note the problems for which the methods developed in this paper are most likely to be useful. These include the use of crossing symmetry to obtain relations between phase contours and zeros of scattering amplitudes, and the study of relations between asymptotic behavior at fixed momentum transfer and at fixed angle. These topics will be developed in more detail in later papers.

2. GENERAL THEOREMS AND SPECIAL ASSUMPTIONS

Our study of phase contours of scattering amplitudes is partly motivated by certain general theorems that relate to high energy behavior. We wish to find how these theorems work out in practice for scattering amplitudes derived from experiment and from simplified models. We also seek an heuristic extension of these theorems to regions where the scattering amplitude is insufficiently understood to permit a rigorous treatment. The theorems that are briefly described here relate to (a) Herglotz functions, (b) power behavior at infinity and asymptotic phases, (c) the phase representation and (d) the reduction of an amplitude to a Herglotz function. A more detailed account of theorems on high energy behavior and references to further papers is given in a book by one of us.[1] The intuitive interpretation of the methods described in this section is postponed to Section 4, after we have discussed a model for a scattering amplitude in Section 3, which is designed to indicate the direction in which we are aiming to use phase contours.

(a) Herglotz Conditions

One of the primary applications of phase contours comes from the fact that they describe an important part of the problem of expressing a scattering amplitude in terms of Herglotz functions. The importance of these functions comes from their bounded asymptotic rate of change.

A function $H(z)$ is Herglotz if it is regular in $\mathrm{Im}(z) > 0$, and is such that $\mathrm{Im}H(z) > 0$ whenever $\mathrm{Im}z > 0$, and $\mathrm{Im}H(x) \geqslant 0$ where x is real.

The property of Herglotz functions that plays a central role in our discussion is that for z complex, $|z| > 1$ and $\epsilon < \arg z < (\pi - \epsilon)$, there exists a positive constant C such that

$$\frac{C}{|z|} < |H(z)| < C|z|. \tag{2.1}$$

For z real an analagous result has been obtained by Jin and Martin,[4] which gives

$$\lim_{x \to \infty} x|H(x)| (\log x)^{\frac{1}{2}} = +\infty \tag{2.2}$$

We will discuss the reduction of a scattering amplitude to a Herglotz function under simplifying assumptions in part (d) of this section, and with special models in Section 4. In the first instance our models will be based on asymptotic power behavior but we will later generalize this to include certain types of entire functions. If a function has asymptotic power behavior, the Herglotz results (2.1) follows trivially from

$$\operatorname{Im} z^{\alpha} = |z|^{\alpha} \sin(\alpha\, \Theta) > 0 \tag{2.3}$$

for $0 < \Theta < \pi$.

The problem of reducing a general function to a Herglotz function is implicitly solved in the phase representation of Sugawara

and Tubis[5] which we consider below. It has also been considered by Kinoshita[6] with certain restrictions on the oscillations of Im F(z). Difficulties associated with the general problem of oscillations have been studied by Eden and Lukaszuk.[7] Although our models will permit certain types of oscillation to continue to infinity we will not consider the associated general problem.

(b) Power Behavior at Infinity

The asymptotic phase of a scattering amplitude can be determined if it is dominated at infinity by a term that is even or odd under crossing and has asymptotic power behavior. This consequence of the Phragmén-Lindelöff theorem was first noted by Meimann,[8] and was further developed by Logunov et al[9] and by Van Hove.[10]

We consider an amplitude that is symmetric (even under crossing, even signature in Regge theory). Then

$$F_S(-w + io, t) = F_S^*(w + io, t), \tag{2.4}$$

where w denotes the symmetric energy variable,

$$w = \frac{1}{2}\left(s - u\right) = s + \frac{1}{2}t - \frac{1}{2}\sum m^2. \tag{2.5}$$

If the energy behavior of $|F_S|$, for fixed t, is given by

$$\left|\frac{F_S(w,t)}{w^\alpha}\right| \to C \quad \text{as} \quad |w| \to \infty, \tag{2.6}$$

where C is a real constant, then the phase can be found from (2.4). This gives

$$F_S(s,t) \sim C \quad w^{\alpha} \exp\left[i\pi\left(1 - \frac{1}{2}\alpha\right)\right]$$

$$\sim C\, s^{\alpha} \exp\left[i\pi\left(1 - \frac{1}{2}\alpha\right)\right], \quad \text{as} \quad s \to \infty. \tag{2.7}$$

Similarly for an antisymmetric amplitude (odd signature),

$$F_A(-w + io,\ t) = -F_A^{*}(w + io,\ t), \tag{2.8}$$

and

$$F_A(s,t) \sim C \exp\left[i\pi\left(\frac{1}{2} - \frac{1}{2}\alpha\right)\right], \quad \text{as} \quad s \to \infty. \tag{2.9}$$

These relations have been generalized for symmetric forward scattering amplitudes to include a wider class of functions that may have quite complicated oscillations. There are two main methods for achieving this generalization, both of which make use of the fact that ImF is non-negative for a forward scattering amplitude. The first of these methods, due to Khuri and Kinoshita,[11] is based on the theory of univalent functions. They derive a wide class of inequalitities between the rate of growth and the phase of a univalent function that is constructed from the symmetric forward amplitude. These inequalities will be of value in later refinements of our discussion in this paper, but they are of a more general nature than we require in our present

simplified study, which is concerned with gross structure, rather than fine structure, of phase and modulus relations.

Rigorous relations involving symmetric scattering amplitudes have also been studied by Jin and MacDowell.[12] Their method is based on the phase representation of a scattering amplitude, that was first introduced by Sugawara and Tubis.[5] We will outline the derivation of the phase representation since the method is closely related to our later procedure.

(c) The Phase Representation

Let $F(z)$ be a scattering amplitude for equal mass particles, that is symmetric under $s \longleftrightarrow u$, where

$$z = \frac{(s-u)^2}{16m^4} = \frac{\left(s + \frac{1}{2}t - 2m^2\right)^2}{4m^4} . \tag{2.10}$$

Then for $-4m^2 < t < 4m^2$, $F(z)$ will have the following properties:

(i) it is analytic in the z plane, cut from z_0 to infinity, where

$$z_0 = \frac{\left(\frac{1}{2}t + 2m^2\right)^2}{4m^4} , \tag{2.11}$$

(for the present we assume that there are no poles),

(ii) $|F(z)| < |z|$ as $|z| \to \infty$,

(iii) $F(z^*) = [F(z)]^*$.

In addition it is assumed that

(iv) for x real greater than z_0, $\mathrm{Im}F(x)$ is continuous and has only a finite number of zeros.

It has been shown by Jin and Martin[13] that such a function has only a finite number of zeros in the cut z plane, at $z_1, z_2, \cdots z_{n'}$ say. Hence $\log G(z)$ is analytic in this plane, where

$$F(z) = \prod_{1}^{n'} (z - z_q)\, G(z). \tag{2.12}$$

The phase $\delta(x)$ of $F(x)$ satisfies

$$\delta(x) = \frac{1}{2i}\left[\log G(x + io) - \log G(x - io)\right] . \tag{2.13}$$

From assumption (iv), $\delta(x)$ is bounded, and since $F(z_0)$ is real we must have $\delta(z_0) = n\pi$ where n denotes zero or an integer (positive or negative). We will find later that it is not always convenient to follow the usual practice of choosing $\delta(z_0)$ to be zero, since this may conflict with our choice of asymptotic phase as in Eq. (2.7), for example.

From properties (i) to (iv) the phase representation of Sugawara and Tubis can be established.[5,12] This is,

$$F(z) = A \exp(in\pi) \prod_{1}^{n'} (z - z_q) \exp\left[\frac{z}{\pi} \int_{z_0}^{\infty} \frac{\delta(x)dx}{x(x - z)}\right] . \tag{2.14}$$

When there is a pole at x_0, this expression gets multiplied by $(z - x_0)^{-1}$.

In order to illustrate the use of the phase representation we specialize to the forward amplitude $(t = 0)$; then the phase must satisfy $0 \leqslant \delta(x) \leqslant \pi$. It has been noted by Jin and MacDowell[12] that the stronger condition

$$0 < \pi\delta_1 < \delta(x) < \pi\delta_2 < \pi, \tag{2.15}$$

combined with the phase representation, leads to the following bound as $z \to \infty$ in any complex direction $(\Theta \neq 0)$ in the physical sheet,

$$C_2|z|^{n_0-\delta_2}\left(\sin\frac{1}{2}\Theta\right)^{(\delta_2-\delta_1)} < |F(z)| < C_1|z|^{n_0-\delta_1}\left(\sin\frac{1}{2}\Theta\right)^{\delta_1-\delta_2}, \tag{2.16}$$

where n_0 denotes the number of zeros minus the number of poles of $F(z)$. Along the real axis, the corresponding results are

$$\frac{F(x)}{x^{p+n_0}} \text{ is integrable when } p > (1 - \delta_1), \tag{2.17}$$

$$\frac{x^{p+n_0}}{F(x)} \text{ is integrable when } p < (-1 - \delta_2). \tag{2.18}$$

If we now make the special assumption of asymptotic behavior like a power as $|z| \to \infty$, we have $\delta_1 = \delta_2$, and as $x \to \infty$,

$$F(x) \sim C\, x^{n_0-\delta_1} \exp(i\delta_\pi) \exp(in_\pi) , \tag{2.19}$$

where C is real and positive. Assuming an asymptotically constant total cross section, we obtain

$$n_0 - \delta_1 = \frac{1}{2} . \tag{2.20}$$

Thus if $n_0 = 1$, we have $\delta_1 = \frac{1}{2}$ and it is consistent to choose $n = 0$ in (2.19). However, if $n_0 = 0$, we obtain $\delta_1 = -\frac{1}{2}$ and for consistency we must choose n to be odd, $n = 1$ say.

(d) Oscillations of $\mathrm{Im}F(x)$

We consider next how the phase representation can be used to remove oscillations of $\mathrm{Im}F(x)$. The aim is to remove polynomial factors (both positive and negative powers) until we obtain a function whose phase satisfies a condition like (2.15).

We assume that the phase $\delta(x)$, of the amplitude $F(x)$, is a continuous function of x. We need to distinguish points, $x = a_n$, at which $\delta(x)$ increases through an integer multiple of π. Similarly, let $x = b_m$ denote points at which $\delta(x)$ decreases through an integer multiple of π.

Define $\eta(x)$ from $\delta(x)$, by adding or subtracting multiples of π, so that

$$0 \leqslant \eta(x) \leqslant \pi. \tag{2.21}$$

To avoid an undue number of alternatives we will suppose that $\delta(z_0) = 0$, in the phase representation (2.14). Suppose also that $\delta(x)$ increases as x increases from z_0, and it passes through π at $x = a_1$, but does not reach 2π. Then

$$\eta(x) = \delta(x) - \pi\Theta(x - a_1), \tag{2.22}$$

where $\Theta(x) = 0$, $x < 0$ and $\Theta(x) = 1$, $x > 0$. From Eq. (2.14) (assuming no zeros or poles) we obtain

$$F(z) = \exp\left[\frac{z}{\pi}\int_{z_0}^{\infty}\frac{\delta(x)dx}{x(x - z)}\right] = \left(\frac{a_1 - z}{a_1}\right)\exp\left[\frac{z}{\pi}\int_{z_0}^{\infty}\frac{\eta(x)dx}{x(x - z)}\right]. \tag{2.23}$$

More generally, we take

$$\eta(x) = \delta(x) - \pi\sum_n \Theta(x - a_n) + \pi\sum_m \Theta(x - b_m). \tag{2.24}$$

This gives

$$F(z) = \exp\left[\frac{z}{\pi}\int_{z_0}^{\infty}\frac{\delta(x)dx}{x(x - z)}\right]$$

$$= \prod_n\left(\frac{a_n - z}{a_n}\right)\prod_m\left(\frac{b_m}{b_m - z}\right) G(z), \tag{2.25}$$

where

$$G(z) = \exp\left[\frac{z}{\pi} \int_{z_0}^{\infty} \frac{\eta(x)dx}{x(x - z)}\right] . \tag{2.26}$$

We will assume power behavior at infinity, then as $|z| \to \infty$,

$$\frac{C_2}{|z|} < |G(z)| < C_1. \tag{2.27}$$

If there are zeros or poles of $F(z)$, these should first be factored out as noted in Eq. (2.14) and in the paragraph following it. Let n_0 denoted the number of zeros minus the number of poles; let $N^{(+)}$, $[N^{(-)}]$ denote the number of points a_n, $[b_n]$, at which $\delta(x)$ increases, [decreases], through an integer multiple of π. Then as $|z| \to \infty$

$$C_2|z|^{p-1} < |F(z)| < C_1|z|^p, \tag{2.28}$$

where

$$p = n^0 + N^{(+)} - N^{(-)}. \tag{2.29}$$

We will later be considering analagous procedures when the scattering amplitude has a branch cut along the entire s axis. In such a case it is necessary to work only in the upper half plane (or lower half). Then it is essential to remove the zeros in $\text{Im}s > 0$ before removing oscillations. This is because the removal of a zero in $\text{Im}s > 0$

(without removal of the associated zero in $\mathrm{Im}s < 0$) introduce an additional oscillation of $\mathrm{Im}F$ on the real axis. In the present section each zero of F in the z plane corresponds to a pair of zeros in the s plane so the problem of coupling between zeros and oscillations does not arise.

3. A PURE REGGE BACKGROUND

We begin our discussion of phase contours with a special model based on Regge theory. We will confine our discussion to a single channel (the s-channel) in which the phase contours are dominated by Regge poles in the other channels even at low energies. We are aware that this model will not represent a situation in which low energy resonances are important and that we may be committing the additional crime of double counting. Resonance interference will be considered in Section 5. However, subject to the validity of our high energy assumptions within Regge theory, we will give reasons for supposing that certain important aspects of the topology of phase contours are given by the Regge background, especially outside the resonance region. For this reason we will consider the topology that arises from several different assumptions about the high energy behavior.

(a) Symmetric Single Pole Exchange

Let $F(s,t)$ be a symmetric scattering amplitude that describes the scattering of equal mass bosons. We consider first the approximation of representing F, in the s- channel, by the superposition of a single Pomeron Regge pole exchange in the t-channel and also one in the u-channel,

$$F(s,t) = b(t)s^{\alpha(t)} \exp\left[i\pi\left\{1 - \frac{1}{2}\alpha(t)\right\}\right] + b(u)s^{\alpha(u)} \exp\left[i\pi\left\{1 - \frac{1}{2}\alpha(u)\right\}\right]. \quad (3.1)$$

In Regge theory it is a usual assumption that such an approximation is valid for fixed t as $s \to \infty$ and for fixed u as $s \to \infty$. We will, however, extrapolate this solution to low energies and will call our extrapolation the Regge background.

It is necessary to specify the dependence of the residue $b(t)$ and the trajectory $\alpha(t)$ on the momentum transfer t. We will consider a variety of possible assumptions beginning with, (i) $b(t)$ is real and slowly varying and non-zero in the range that is considered, (ii) $\alpha(t)$ decreases monotonically as t decreases and has no lower bound, with $\alpha(0) = 1$ so as to give an asymptotically constant total cross section.

The phase $\phi(s,t)$ is defined so that,

$$F(s + io, t) = |F(s,t)| \exp[i\phi(s,t)]. \tag{3.2}$$

The asymptotic phase for $t = 0$, as s tends to $+\infty$ along the real axis $(s + io)$ is chosen to be $1/2\,\pi$ (rather than $1/2\,\pi + 2n\pi$). This is the usual convention in Regge theory, and gives $\phi \to +3/2\,\pi$, as $s \to -\infty$ along $(s + i0)$. For $t \neq 0$ the phase of F as $s \to \infty$ will be given by

$$\phi(s,t) \sim \pi \left[1 - \frac{1}{2}\alpha(t)\right]. \tag{3.3}$$

Phase contours in the real (s,t) plane are defined as the curves of constant phase. They are illustrated, for this model of a Regge background, in Figure 3.1. We have shown the phase contours

$\mathrm{Re}F = 0$, which are separated by contours $\mathrm{Im}F = 0$. The oscillations of the contours in this figure are due to the simplicity of the model and, if they occur in a more realistic model, one would expect them to be very small. However, oscillations will, in general, arise from other sources (as we see later), so we will take them into account in the following discussion.

The topology of the phase contours, shown in Figure 3.1, is more generally typical than one might expect from our special model. Given the assumptions of Pomeron dominance and a continuously falling trajectory $\alpha(t)$ for decreasing t, we note the following consequences:

(i) Phase contours are asymptotically constant, parallel to $t = \text{const.}$ or to $u = \text{const.}$

(ii) The phase contours $\mathrm{Im}\phi(s,t) = 0$ cannot cross the line $t = 0$ or the line $u = 0$ above the elastic threshold $s = 4m^2$. This follows from the optical theorem and the positivity of the total cross section associated with a symmetric (even signature) amplitude.

(iii) We expect phase contours to be continuous, except possibly at divergent singularities of the scattering amplitude. There are no such singularities in the physical region. It follows that the phase contour $\phi = -n\pi/2$, that is asymptotically parallel to $t = \text{const.}$, must connect to the contour $\phi = -n\pi/2$ that is asymptotically parallel to $u = \text{constant}$.

(iv) Phase contours can cross each other only at zeros of the scattering amplitude. On a given contour the phase changes by $\pm\pi$ as

it crosses other contours. In this case the zeros of $F(s,t)$ would be in the real (s,t) plane. We will see in Section 5 that such zeros may arise if we superimpose a resonance on a Regge background, and in Section 7 we will see that real zeros occur, for physical values of s and t, in pion-nucleon scattering amplitudes.

It is tempting to assume that zeros of an amplitude will not occur for physical values of s and t except at low energies or medium energies, where resonances are strong relative to the background, but we do not know that this is true in practice and will not assume it in general. However, it is more reasonable to suppose that any given phase contour will not encounter more than a finite number of zeros.

The principal modifications to Figure 3.1, that we would expect in a more realistic model are in the low energy region where there may be zeros, and closed loop contours may develop. In addition, they will change if we have different asymptotic conditions. These will be studied later in this section.

(b) Zeros of ImF

In our model $\mathrm{Im}F \to 0$, as $s \to \infty$ for fixed t, when $\alpha(t) = 0, -2, -4, \cdots$. Thus, if we take a value t_n of t such that

$$-2n < \alpha(t_n) < 2 - 2n, \tag{3.4}$$

then, for large fixed s, $\mathrm{Im}F(s,t)$ will have n zeros in the range

$$0 > t > t_n. \tag{3.5}$$

Now consider $F(s,t_n)$ in the complex s plane. Along the real axis $\mathrm{Im}F(s,t_n)$ will have at least n zeros, at the intersections with the constant phase contours

$$\phi(s,t) = \gamma\pi, \quad \gamma = 1,2,\cdots n. \tag{3.6}$$

The case $n = 2$ is illustrated in Figure 3.2(a)(b). As s varies along $s + io$ from $s_0 = 4 - t_n$, to ∞ in Figure 3.2(a), the phase and modulus of $F(s,t_n)$ varies as indicated in Figure 3.2(b).

When there are no zeros of $F(s,t_n)$ for complex s, the number n of effective intersections with $\mathrm{Im}F = 0$ corresponds to the asymptotic power s^{α} according to the inequality (3.4). If we consider the whole real axis $-\infty$ to ∞, $\mathrm{Im}F(s + io, t_n)$ will have 2n effective zeros.

In Figure 3.2(c) and (d), we show the corresponding behavior of $F(s,t_n)$, when there are ineffective intersections with the phase contour $\phi = 2\pi$. Double (or even number) intersections of this type do not contribute to the asymptotic power of s. This is a simple example of the situation considered in Section 2(d) when we modified the phase representation. It is interesting to note that for $\alpha(t_n)$ exactly equal to -2, there will be an infinite number of ineffective intersections even in this very simple example. Correspondingly our method of Section 2(d) would introduce the ratio of two entire functions of the same order and type.

(c) Regge Pole Correction Terms

For high energies the term given by the leading Regge trajectory is assumed to dominate over the correction terms given by other

trajectories and the background integral. However, these terms will be larger than those from crossed channel trajectories so that the small oscillations of phase lines that we considered in the last section will become modified. For example, if we choose t_n so that

$$\alpha_1(t_n) = -2n$$

for the leading trajectory, we will have the following contributions from the first and second trajectories in the t channel,

$$F(s,t_n) \sim (-1)^{n+1} s^{-2n} b_1(t_n) + \left[-\exp(-i\pi\alpha_2/2)\right] s^{\alpha_2(t_n)} b_2(t_n) \tag{3.7}$$

Hence, for large s,

$$\phi(s,t_n) \sim (n+1)\pi + \frac{b_2(t_n)}{b_1(t_n)} s^{\alpha_2+2n} (-1)^{n+1} \sin\left[\pi\alpha_2(t_n)/2\right] \tag{3.8}$$

where $(\alpha_2 + 2n) < 0$. Thus as $s \to \infty$ the phase difference from $(n+1)\pi$ tends to zero but has a constant sign, as is well known. However, the significant point that we wish to note, is the dominance of this phase correction term over the correction due to the u-channel pole. This dominance will make finite the number of intersections of the phase line $\phi(s,t) = (n+1)\pi$ with any fixed line $t = t_n$. Thus the method of Section 2(d) for removing oscillations will not introduce entire functions, but only the ratio of polynomials in s.

At low energies we would, in general, expect the phase contours to be distorted by resonances. Equivalently they could in principle be represented by Regge poles plus the background integral. However, there is no inconsistency evident at this stage of our discussion in assuming a weak resonance situation in the s-channel, so that the Regge background dominates in determining phase contours even at low energy.

(d) Zeros of Residues

If the residue $b(t) = 0$, whenever $\alpha = -(2n + 1)$, then the phase of the t-channel Regge term in Eq. (3.1) is no longer given by Eq. (3.3). Its value depends on the phase of the correction terms that come from other t-channel Regge poles. Suppose, for example, that these terms are real and positive when $t = t_n^0$, where

$$\alpha(t_n^0) = -(2n + 1). \tag{3.9}$$

Then the phase along $s + i0$ for $s \to +\infty$ will be given by

$$\phi(s,t) = \pi[1 - \alpha(t)]. \tag{3.10}$$

The phase for $s \to -\infty$ will depend on the route taken from large real $s > 0$ to large real $s < 0$. If the route is asymptotic along $s = K\exp i\theta$, with K large, the phase change will be $\alpha\pi$. Other routes give a change that depends on the location of complex zeros of the amplitude. We will consider this in more detail in the next paper.

Typical phase contours in the s-channel, when $b(t)$ is zero for $t = t_n^0$, are shown in Figure 3.3(a). In Figure 3.3(b) the corresponding behavior of $F(s,t_1^0 + \epsilon)$ is shown for s real $(4m^2 - t_1 < s < \infty)$.

In principle such violent phase fluctuations as t decrease through t_1^0 would be observable experimentally through corresponding fluctuations in the polarization. We will see in Section 8 that zeros of the P' exchange Regge term (a non-leading term) also cause fluctuations of phase contours like those illustrated in Figure 3.3(a), (see Figure 8.2 showing phase contours for $B^{(+)}$ in pion-nucleon scattering). In suitable circumstances these fluctuations should be observable in sufficiently accurate experiments on polarization, for example in pion-nucleon scattering in the energy range $T_\pi = 4$ to 6 Gev with $0.4 < (-t) < 1.2\ (\mathrm{GeV})^2$.

(e) A Fixed Pomeranchuk Pole

If the leading Regge pole for $t \leq 0$ is fixed at $\alpha_1(t) = 1$, there will be striking and significant differences in phase contours from those discussed above. For any fixed $t < 0$, we would have

(i) The asymptotic phase $\phi(s,t) \sim 1/2\ \pi$.

(ii) The asymptotic rate of change of $|F|$ will be the same as $|s|$.

These conditions mean that only the phase contour $\phi(s,t) = (1/2)\pi$ can be asymptotically parallel to $t = 0$. This does not necessarily imply that other phase contours will close at finite values of s. For example, consider the model,

$$F(s,t) = b_1(t) i\ s + b_2(t) \exp[-i\pi\alpha_2(t)/2] s^{\alpha_2}$$

$$+ b_1(u) i\ s + b_2(u) \exp[-i\pi\alpha_2(u)/2] s^{\alpha_2}, \qquad (3.11)$$

If

$$\frac{b_2(t)}{b_1(t)} \left| \frac{2t}{1 - z_0} \right|^{\alpha_2(t)-1} \longrightarrow C, \quad \text{as} \quad t \to \infty, \tag{3.12}$$

where C is a finite constant and $z_0 = \cos \Theta_0$, the phase at an angle Θ_0 will not tend to $1/2\,\pi$ as s (or t) tends to infinity. At smaller angles than Θ_0 the phase $\phi(s,t)$ always tends to $1/2\,\pi$. This situation is illustrated in Figure 3.4(a), when (3.12) holds. In Figure 3.4(b) we show the situation when the Pomeranchuk pole dominates at all angles ($C = 0$, when $z_0 = 0$).

(f) Mandelstam-Regge Branch Cuts

A similar situation to that for a fixed Pomeranchuk pole may be expected from the assumption of Mandelstam-Regge branch cuts. Although the leading cut is fixed at $\ell = 1$, for $t < 0$, it is plausible that the discontinuity could be small. We will estimate the effect of branch cuts from a crude model for the strengths of their discontinuities.

Consider a branch cut that arises from the exchange of N Pomeranchuk poles $\alpha(t)$, (Mandelstam[14]). The location of the branch point is given by

$$\alpha_c^{\,N}(t) = \text{Max}\,[\,\Sigma\{\alpha(t_r) - 1\} + 1] \tag{3.13}$$

subject to

$$\sum (-t_r)^{\frac{1}{2}} = (-t)^{\frac{1}{2}}. \tag{3.14}$$

The value of α_c will depend on the form of the Pomeranchuk trajectory $\alpha(t)$. We will assume that this is such that

$$\alpha_c^N(t) = \sum \{\alpha(t/N^2) - 1\} + 1. \tag{3.15}$$

Since the branch cut arises from the exchange of N Pomeranchuk poles, we assume that its discontinuity, b_c^N is related to the residue $b(t)$ at a Pomeranchuk pole by

$$b_c^N(t) \approx [b(t/N^2)]^N. \tag{3.16}$$

To illustrate the effect of such branch cuts, we take

$$b(t) \sim \exp[-(-t)^\gamma], \quad \text{for} \quad t \ll 0. \tag{3.17}$$

Then

$$b_c^N(t) \sim \exp[-N(-t/N^2)^\gamma]. \tag{3.18}$$

In the special case $\gamma = 1/2$,

$$b_c^N(t) \sim \exp[-(-t)^{\frac{1}{2}}]. \tag{3.19}$$

Then the branch cut, for large $|t|$ $(t < 0)$, will have a discontinuity for any N, whose magnitude is comparable with the residue at the Pomeranchuk pole.

For a general value of γ we can investigate the asymptotic form of the phase contours by considering the ratio (compare with (3.12)),

$$\frac{b(t)}{b_c^N(t)} \sim \exp\left[\left\{N^{1-2\gamma} - 1\right\}(-t)^{\gamma}\right], \quad N > 2, \tag{3.20}$$

For $\gamma < 1/2$ this ratio always satisfies the conditions for phase contours to be "open", (compare with Eq. (3.12)). They would have the general form

$$t = -A\left[\alpha_c(t) - \alpha(t)\right]^{1/\gamma} (\log s)^{1/\gamma} \tag{3.21}$$

For $\gamma > 1/2$, our estimated branch cut discontinuity, $b_c^N(t)$, decreases more slowly with t than the residue $b(t)$. As $N \to \infty$, $b_c^N(t) \to 1$, for any fixed t. Thus, the leading branch cut (at $\alpha_c = 1$) would dominate for large enough values of s. Then all phase contours in $t < 0$ would close, as indicated in Figure 3.4(b).

4. OSCILLATIONS, ZEROS AND HERGLOTZ CONDITIONS

In this section we give an heuristic discussion of how zeros and oscillations of ImF are related to asymptotic behavior. In particular, we wish to see how the essential features of the theorems considered in Section 2 are related to the topology of phase contours. The latter will be considered both in the real (s,t) plane, as in Section 3, and in the complex s plane. Our aim is to see what aspects of phase contours are crucial to high energy behavior and what aspects are not directly significant.

We begin by noting some results on zeros and oscillations that follow from dispersion relations. We then consider how the zeros of ImF are related to high energy behavior and to the zeros of F itself. Next we note how zeros of F affect the values of the phase $\phi(s,t)$. Then we summarize the points relating to the removal of zeros and oscillations so as to express F in terms of a Herglotz function.

(a) Dispersion Relations and Oscillations

Let $F(z,t)$ be a function that satisfies an unsubtracted dispersion relation for a given value of t,

$$F(z,t) = \frac{1}{\pi}\int_a^{\infty} \frac{dx\,\mathrm{Im}F(x,t)}{x - z} + \frac{1}{\pi}\int_{\infty}^{-b} \frac{dx\,\mathrm{Im}F(x,t)}{x - z} \tag{4.1}$$

Our assumption requires that $F \to 0$ as $|z| \to \infty$. If $\mathrm{Im}F(x,t) > 0$, for x real along $x + i0$, we see that

$$\mathrm{Im}F(z,t) > 0, \qquad \text{for } \mathrm{Im}z > 0. \tag{4.2}$$

Hence $F(z,t)$ is Herglotz and, using also our assumption that (4.1) converges,

$$\frac{C_1}{|z|} < |F(z,t)| < C_2 \tag{4.3}$$

as $|z| \to \infty$, where C_2 may be as small as we please.

If we have power behavior asymptotically,

$$|F(z,t)| \sim |z|^{\alpha(t)} \quad \text{as} \quad |z| \to \infty, \tag{4.4}$$

then $-1 < \alpha < 0$ if (4.1) and (4.2) hold. If $\alpha < -1$ we can write a superconvergence relation,

$$\int_{-\infty}^{\infty} \mathrm{Im}F(x,t)dx = 0. \tag{4.5}$$

It follows that $\mathrm{Im}F(x,t)$ must change sign at least once along the real x axis. By forming higher moments we see that $\mathrm{Im}F$ must change sign at least N times when $\alpha < -N$.

If $\alpha > 0$, we cannot use an unsubtracted dispersion relation for $F(z,t)$. There may be complex zeros of F and/or real zeros of $\mathrm{Im}F$; we consider these possibilities next.

(b) Zeros of ImF

We assume that F is antisymmetric (odd signature) and has power behavior at infinity. Then for $|s|$ large,

$$F(s,t) \sim |s|^{\alpha} \exp i \left[\frac{\pi}{2} + \alpha\left(\Theta - \frac{\pi}{2}\right)\right] , \tag{4.6}$$

where Θ denotes arg s. This defines the mapping of the contour C_s in the s-plane to C_F in the F plane, where C_s denotes: $|s|$ fixed and large, $0 \leqslant \Theta \leqslant \pi$, (see Figure 4.1(a)). When

$$-2n -1 < \alpha < -2n, \tag{4.7}$$

the contour C_F will encircle the origin clockwise, n times, as indicated in Figure 4.1(b). Thus ImF will have 2n zeros. If α corresponds to a positive power C_F will be traced anticlockwise, but (as we see later) F must then have complex zeros. If F has even signature, in the figure (b) the contour C_F should be rotated through $\pi/2$ (anticlockwise).

Now consider the mapping $s \to F$, as C_s is deformed into C_s' in Figure 4.1(a), where C_s' lies along $s + i0$, with s real. Denote the mapping of C_s' into the F plane by C_F'.

If $F(s,t) \neq 0$ in $\mathrm{Im}s > 0$, C_F will be deformed into C_F' without crossing through the origin. The total number of times C_F' encircles the origin will be the same as for C_F. Unfortunately extra zeros of ImF on the contour C_F' may be introduced during the deformation from the contour C_F. This is because, for finite values of s, the amplitude F may no longer be dominated by the term shown in Eq. (4.6). Thus, for example, the curves C_F' shown in

Figure 4.1 (c) and (d) would correspond to the same asymptotic behavior.

We would expect "ineffective" zeros of ImF, of the form shown in Figure 4.1(d), to be indicated by the form of the phase contours. Consider a particular contour

$$\phi(s,t) = n\pi \tag{4.8}$$

on which ImF = 0. Let its real section include the curve shown in Figure 4.2(a). We will study its complex section for different values of t.

Let t_1, t_2, t_3 be the values of t giving the lines shown in Figure 4.2(a). The asymptotic phase contours can be determined from Eq. (4.6), which gives

$$\phi(s,t) = \frac{1}{2}\pi(1 - \alpha) + \alpha\Theta, \tag{4.9}$$

for $s = K \exp(i\Theta)$, with K large and positive. Since ϕ increases monotonically with Θ, it is clear that the value $\phi = n\pi$ can be reached only once. For $t = t_3$ and s complex, there is a curve on $\phi(s,t_3) = n\pi$ through each of the real points s_1, s_2, s_3 indicated in Figure 4.2(a). This curve can go to infinity in Ims > 0 only once. Hence its general form must be that shown in Figure 4.2(b). The corresponding complex sections of the phase contours (4.8) for $t = t_2$ and $t = t_1$ are shown in Figure 4.2(c) and (d). Only the parts reached

from $\mathrm{Im}s > 0$ are shown, so the broken lines will correspond to the phase contour on a second sheet, through a branch cut in general.

This discussion shows that if an amplitude $F(s,t)$ is bounded by some power of s at infinity, for $t = t_0$, this power is directly related to the number of real phase contours, $\phi(s,t) = n\pi$, that are intersected an odd number of times by the line $t = t_0$. Each phase contour corresponds to an extra power of plus or minus one, depending on whether the phase is decreasing or increasing as s passes through the right most intersection. A phase contour, $\phi = n\pi$, that has an even number of intersections with $t = t_0$, can be ignored when determining the nearest integer power of s in $F(s,t_0)$, as $s \to \infty$. Hence the phase contours shown in Figure 3.1, for example, can be used to determine the power behavior for large s; but for fixed s and large t they do not contribute to the power behavior, since $s = s_0$ intersects each contour an even number of times.

Finally we note than an effective zero, of $\mathrm{Im}F(s,t)$ in the real axis, can appear as t varies, only by moving in from infinity in the s plane. This follows from the continuity of the phase contours, so that $\mathrm{Im}F(s,t) = 0$ can meet s real in an odd number of points, only if one point has moved in from infinity. The phase contour in the (s,t) plane, $\phi(s,t) = n\pi$, must therefore by asymptotic to t = constant, as in Figure 4.3(a). The corresponding phase contour in the s plane, as t decreases by ϵ, will cut off the corner of the large semicircle in $\mathrm{Im}s > 0$, as indicated in Figure 4.3(b).

(c) Zeros of F

When $F(s,t)$ has zeros in the complex s plane for some value of t, the standard procedure mentioned in Section 2 is to remove the zeros by dividing them out of F to give a new function G that is free from complex zeros,

$$G(s,t) = \frac{F(s,t)}{\prod\left[s - s_r(t)\right]} . \tag{4.10}$$

However, since we will be concerned with the use of phases to obtain a self consistent topology of phase contours for the amplitude F itself, it is necessary to obtain an intuitive picture of the effects of zeros.

The phase of $F(s,t)$ will depend on the route taken from the asymptotic region for forward scattering where the phase is first defined, to the point (s,t). Similarly the phase change of F from $s + i0$ to $-s + i0$ as $s \to \infty$, depends on whether we follow the circle at infinity or move along the real axis. The former path goes above the zeros and the latter below them. The phase difference for the two paths will be

$$\Delta\phi(t) = 2n\pi \quad , \tag{4.11}$$

where n denotes the number of zeros in $\mathrm{Im}\, s > 0$.

We have seen that for a symmetric amplitude,

$$F(s,t) \sim |s|^{\alpha} \exp\left[i\left\{\pi - \alpha\left(\frac{\pi}{2} - \theta\right)\right\}\right], \tag{4.12}$$

where $\Theta = \arg s$. The phase change along C_s in Figure 4.1(a) from 1 to 3 will be

$$\phi_3 - \phi_1 = \alpha\pi, \qquad \text{path } C_s. \tag{4.13}$$

However, if there are n zeros in $\mathrm{Im}s > 0$, the phase change, from 1 to 3 along C_s' in Figure 4.1(a), will be

$$\phi_3 - \phi_1 = \alpha\pi - 2n\pi. \tag{4.14}$$

The case $\alpha = -(2 + \epsilon)$, with $0 < \epsilon < 2$ and $n = 1$, is illustrated in Figure 4.4(a) and (b). To deform from C_s to C_s' we must pull the contours across one zero of F. Thus the path of F in diagram (b) changes from one with effective oscillations of $\mathrm{Im}F$ to a path with ineffective oscillations.

(d) Herglotz Conditions

A symmetric amplitude (even signature) has at least one change of sign along $s + i0$ (in general there must be an odd number of changes). We can readily remove one oscillation, by multiplying by $\left[(s - 4m^2)s\right]^{\frac{1}{2}}$ in the case of the forward amplitude, for example. Alternatively we could consider the number of sign changes of $\mathrm{Re}F$, since (except for the forward amplitude) there is no special advantage from working with $\mathrm{Im}F$ except that it is conventionally used in Herglotz conditions. We summarize the results of removing zeros and oscillations to give a Herglotz function. Let

$$|F(s,t)| \sim |s|^{\alpha(t)} \quad \text{as} \quad s \to \infty. \tag{4.15}$$

For a symmetric amplitude, along $s = |s|\exp(i\Theta)$, $0 < \Theta < \pi$,

$$\pi - |\alpha|\frac{\pi}{2} < \phi(s,t) < \pi + |\alpha|\frac{\pi}{2} \tag{4.16}$$

For an antisymmetric amplitude,

$$\frac{\pi}{2} - |\alpha|\frac{\pi}{2} < \phi(s,t) < \frac{\pi}{2} + |\alpha|\frac{\pi}{2}. \tag{4.17}$$

Let $\alpha = -(N + \epsilon)$, where $0 \leqslant \epsilon < 1$, and let there be n zeros of F for complex s in $\mathrm{Im}\, s > 0$, (exceptionally there may be real zeros but we choose t to avoid these). In general there will also be n zeros at conjugate points in $\mathrm{Im}\, s < 0$.

Along $s + i0$ there will be a phase change from $s = +\infty$ to $s = -\infty$,

$$\Delta\phi = \alpha\pi + 2n\pi. \tag{4.18}$$

In practice the factor $\alpha(t)$ is expected to change continuously with t, but $n(t)$ will change discontinuously as new zeros enter the half plane $\mathrm{Im}\, s > 0$. These zeros may enter either at infinity, or at a singularity, or at a regular point. The conjugate zero will simultaneously enter the lower half plane. A knowledge of the effective oscillations, and effective zeros, permits a reduction of F to a function satisfying the Herglotz conditions.

5. RESONANCE TERMS AND INTERFERENCE EFFECTS

In this section we study zeros and phase contours for several interference models, and we relate the special results to the general conclusions suggested by examples in the previous section and by the theorems mentioned in Section 2. We emphasize that we do not know a correct prescription for combining resonances with a background term. It is unlikely that there is a "best" method for separating resonances and a background. Thus our procedure in this section is concerned with phase contours in models which are not realistic but may throw light on an improved approach to the problem of resonance interference.

We consider first a simple D state resonance plus constant background and locate the zeros. Next we consider how a variation of parameters in a model can cause a real zero to become complex. Then the zeros in the D-state resonance model are related to the asymptotic behavior in the t-channel and in the s-channel. We study also the manner in which phase contours intersect at a zero of the amplitude. We then give examples of phase contours in a model given by a resonance plus a Regge gackground.

(a) Zeros for a Resonance Model

We consider a D state resonance with a slowly varying background,

$$F(s,t) = f(s)P_2(z) + B + iB', \tag{5.1}$$

where

$$z = \cos\Theta = 1 + \frac{2t}{s - 4m^2} . \tag{5.2}$$

Note that this differs from the variable z used in Section 2. The partial wave component, omitting slowly varying factors is taken to be

$$f(s) \simeq \frac{A - s}{(s - A)^2 + \Gamma^2} + \frac{i\Gamma}{(s - A)^2 + \Gamma^2} , \tag{5.3}$$

Initially we fix s at the resonance value, $s = A$, and consider F in the complex z plane. Writing $C = (2\Gamma)^{-1}$,

$$\begin{aligned} F(s,t) &= iC(3z^2 - 1) + B + iB' \\ &= iC\left[3(x^2 - y^2) - 1\right] - 6Cxy + B + iB'. \end{aligned} \tag{5.4}$$

The real and imaginary parts in the z plane are harmonic functions given by

$$X_z = -6Cxy + B, \tag{5.5}$$

$$Y_z = C\left[3(x^2 - y^2) - 1\right] + B'. \tag{5.6}$$

The phase contours in the complex z plane have two possible configurations, which are shown in Figure 5.1(a) and (b). These depend on

whether $(B' - C)$ is negative or positive. The phase $\phi(z)$ is ambiguous in that it depends on whether the zeros are encircled in a clockwise, or an anticlockwise, sense. These ambiguities are of great importance and will be discussed again later. Thus in Figure 5.1(a) and (b) we draw the contours

$$X_z = 0, \quad \phi = 0 \pm \pi, \tag{5.7}$$

$$Y_z = 0, \quad \phi = \tfrac{1}{2}\pi \pm \pi. \tag{5.8}$$

There are two zeros, since $P_2(z)$ is of second order in z. Thus, one zero in $\mathrm{Im}z > 0$ may be expected to correspond to a power law z^2 for large $|z|$, since in general there will be a corresponding zero in $\mathrm{Im}z < 0$ for the functions that we consider.

When s is not at the resonance value, $f(s)$ will not be pure imaginary. We write

$$f(s) = |f|\exp\left\{i\theta(s)\right\}. \tag{5.9}$$

There are two effects that modify the contours shown in Figure 5.1. Firstly, $|f|$ decreases relative to the background term $B + iB'$, as we move away from the resonance. This may effect the inequality $(B' - C) > 0$ and change the contours from those in diagram 5.1(b) to those in 5.1(a). Secondly, the relative phase, of the resonance and background terms, changes. We write

$$B + iB' = b \exp(i\gamma). \tag{5.10}$$

Then

$$F(s,t) = \exp\left\{i\left(\Theta - \frac{\pi}{2}\right)\right\}\left[|f|i\left\{3(x^2 - y^2) - 1\right\} - 6|f|xy + b \exp i\left(\gamma - \Theta + \frac{\pi}{2}\right)\right]. \tag{5.11}$$

When $\Theta = \gamma$, the zeros of F in the z plane lie on $xy = 0$. They will be real if, for the corresponding value f_γ of $|f|$,

$$b - f_\gamma < 0. \tag{5.12}$$

A typical form of this solution is shown in Figure 5.2.

If the resonance parameters are varied, the two solutions of $F(s,t) = 0$, in the z plane, will remain real until $b = f_\gamma$, when they coincide at $z = 0$. For smaller values of f_γ they become complex. This is a general feature, and it is useful in comparing different approximate solutions for a scattering amplitude F (see the discussion following in (b) and Section 7). We will consider the phase contours with resonance interference for real s and real t later in this section.

(b) Real and Complex Zeros

We give a plausibility argument for the following theorem: If two amplitudes are related analytically to each other by a variation

of their parameters (either resonance or background parameters), real zeros in the z-plane (z now denotes any variable in F) can become complex only when they meet in pairs.

Consider the curves

$$\mathrm{Im}F(z,s,b) = 0, \qquad \mathrm{Re}F(z,s,b) = 0, \tag{5.13}$$

in the complex z plane, where b denotes one or more variable parameters. They will meet, in general, at a number of complex points, one of which we denote by

$$z = z_0(s,b). \tag{5.14}$$

When s varies (in one dimension), the zero $z_0(s,b)$ describes a curve in the z plane. From the implicit function theorem, this will be an analytic curve if F is analytic. Hence we can go from the situation indicated by the continuous curve in Figure 5.3(a) to the broken curve, by variation of b, only via a situation in which the two real zeros meet before becoming complex. An alternative variation is shown in Figure 5.3(b) and gives the same conclusion. The curves indicate how $z_0(s)$ moves as s varies through real values. Thus Figure 5.3(a) could be approximated by

$$z_0 = (x_0 + iy_0) = \left[2as + i(s^2 - b)\right]. \tag{5.15}$$

When $b > 0$, there are two real solutions to $\mathrm{Im}z_0 = 0$, namely, $s_0 = \pm(b/a)^{\frac{1}{2}}$. However, for $b < 0$, either z_0 is complex or s_0 is complex. We will see later in this section how the corresponding phase contours appear in the real s, real t plane in these two situations (see Subsection 5(e)).

(c) Zeros and Asymptotic Behavior

We assume that B and B', in our model, behave like constants for large $|z|$ in the physical sheet,

$$F(s,t) = f(s)P_2(z) + B + iB'. \tag{5.16}$$

For fixed s, the large $|z|$ behavior of $F(s,t)$ can be attributed to the two zeros z_1, z_2, which we assume to be located as in Figure 5.1(b). Our general method of converting F to a Herglotz function consists of factoring out the zeros in $\mathrm{Im}z > 0$, and then removing oscillations of the resulting function along z real.

We will see how this procedure works in our model, for which $\mathrm{Im}z_1 > 0$, but $\mathrm{Im}z_2 > 0$ and $\mathrm{Im}F$ is positive along the real axis (Figure 5.1(b)). For $z = x$,

$$\mathrm{Im}F(s,t) = \left[\mathrm{Im}f(s)\right] P_2(x) + B' > 0. \tag{5.17}$$

Consider the function

$$G(z) = \frac{F(s,t)}{z - z_1}. \tag{5.18}$$

Writing γ for the phase of F, and Θ for the phase of $(z - z_1)$, we see that

$$G(z) = \left| \frac{F}{(z - z_1)} \right| \exp i(\gamma - \Theta). \tag{5.19}$$

By assumption (5.17), $0 < \gamma < \pi$, and Θ varies from $-\pi$ to 0 as z varies from $-\infty$ to $+\infty$ along the real axis. Hence $(\gamma - \Theta)$ goes through zero $(2n + 1)$ times along the real axis. Let us take $n = 0$ initially, and let z_0 (real) be the single zero of $\mathrm{Im}G$ for z real. Then we obtain a Herglotz function by writing

$$H(z) = \frac{G(z)}{(z - z_0)} = \frac{F(s,t)}{(z - z_1)(z - z_0)} \tag{5.20}$$

More generally if $n > 0$, we will have $2n$ ineffective zeros of $\mathrm{Im}G$, and our Herglotz function will have the form

$$H(z) = \frac{F(s,t)}{(z - z_1)(z - z_0)} \prod_{i=1}^{n} \left(\frac{z - \alpha_i}{z - b_i} \right) . \tag{5.21}$$

The point that we wish to note from this example, is that a single zero in $\mathrm{Im}z > 0$, for an even function of z, corresponds to a power behavior of degree two for large $|z|$. We will consider a generalization of this example to a Reggeized resonance in Section 6.

(d) Poles and Zeros

For fixed s and large $|t|$, the asymptotic conditions are the same as for large $|z|$ and the relation to zeros is the same. However,

for fixed t and large $|s|$,

$$P_2(z) \sim 1, \qquad |f(s)| \sim |s|^{-1}. \tag{5.22}$$

Hence F will be dominated by $B + iB'$, on our assumption that this is asymptotically constant. We will consider how the zeros of F in $\mathrm{Im}s > 0$ are related to this asymptotic behavior.

By construction $f(s)$ has no poles or zeros in $\mathrm{Im}s > 0$ (our model is over-simplified in this respect since $f(s)$ does not contain the usual Riemann sheet structure). There are no zeros of $\mathrm{Im}f(s)$, so it is a Herglotz function. We can deal with the zeros of F defined by Eq. (5.1) as before, but there is now a double pole at $s = 4m^2$ due to the transformation $z \to s$. Taking this into account, we obtain an s-plane Herglotz function from F, namely for fixed t,

$$H(s,t) = \frac{F(s,t)(s - 4m^2)^2(s_0 - 4)(s_1 - 4)}{4t^2\left[(s - s_0)(s - s_1)\right]} \tag{5.23}$$

where s_0 and s_1 denote the two points (real and complex), that correspond to z_0 and z_1. The double pole is, of course, a non-realistic feature of our model but it illustrates the compensating effects of poles and zeros on high energy behavior and on phase contours. As s moves along (just above) the real axis from $-\infty$ to ∞ the amplitude $F(s,t)$ makes a circuit (-2π) round the origin due to the double pole, which cancels the phase change of π from each of the zeros at $s = s_0$ and $s = s_1$.

(e) Phase Contours Near a Zero and Near Pairs of Zeros

We have noted in part (a) of this section, the ambiguity in phase, for a phase contour that goes through a zero of the amplitude. Now we consider the topology of phase contours in the real (s,t) plane near a zero. Let F be zero at the real point (s_0,t_0). Then, assuming analyticity in the neighborhood,

$$F(s,t) = (s - s_0)\left(\frac{\partial F}{\partial s}\right)_0 + (t - t_0)\left(\frac{\partial F}{\partial t}\right)_0 + \cdots \tag{5.24}$$

$$= (s - s_0)a \exp(i\Theta) + (t - t_0)b \exp(i\psi) + \cdots \tag{5.25}$$

$$= |F| \exp\left[i\phi(s,t)\right] . \tag{5.26}$$

Consider the phase ϕ along a line in the (s,t) plane,

$$t - t_0 = \mu(s - s_0), \tag{5.27}$$

and assume $a > 0$, $b > 0$. Then (see Figure 5.4),

$$\tan \phi(\mu) = \frac{a \sin \Theta + \mu b \sin \psi}{a \cos \Theta + \mu b \cos \psi} . \tag{5.28}$$

As μ varies from $-\infty$ to ∞, $\phi(\mu)$ varies in the range

$$\psi - \pi < \phi(\mu) < \psi . \tag{5.29}$$

These phase contours correspond to phase lines that emerge from a semi-circle round the zero (s_0,t_0) in the real (s,t) plane. The other half of the circle centered on (s_0,t_0) will contain the continuations of these phase contours through the zero at s_0,t_0, each with phase change $\pm\pi$, depending on whether the zero is avoided by an anticlockwise or a clockwise detour. The geometric interpretation of the above discussion and the resulting phase contours near a zero are illustrated in Figure 5.4.

Noting that a range 2π of phase contours must be involved when we make a single circuit of one zero, we can readily extrapolate to the situation when there are two real zeros near to each other. From this we can extrapolate to the case of two coincident zeros, and then to two neighboring complex zeros. The resulting phase contours are illustrated in Figure 5.5.

(f) Phase Contours in a Model: Resonance and Regge Background

One of our objectives in developing the use of phase contours is to contribute to the solution of the problem of combining the asymptotic solutions of Regge theory with the low energy solutions of Resonance models. As a first orientation on this problem we will consider the phase contours that arise from interference between various combinations of the following terms:

(1) Pure Regge background type (1), Pomeranchuk exchange dominates in both forward and backward directions,

$$F_1(s,t) = \left[-(\alpha + 1)(\alpha + 3)s^{\alpha} \exp(-i\pi\alpha/2)\right] + \left[-(\beta + 1)(\beta + 3)s^{\beta} \exp(-i\pi\beta/2)\right] \tag{5.30}$$

where

$$\alpha = \alpha(t) = 1 + (0.5)t, \tag{5.31}$$

$$\beta = \beta(u) = 1 + (0.5)u. \tag{5.32}$$

We have included residue factors that are zero at negative odd integers, but they are not very important in the interference region that we will consider in this section, (but see Section 3(d)).

(2) Pure Regge background type (2), Pomeranchuk exchange dominates forward but an odd signature term dominates backward scattering,

$$F_2(s,t) = \left[-(\alpha + 1)(\alpha + 3)s^{\alpha} \exp(-i\pi\alpha/2)\right] + \left[\beta(\beta + 2)(\beta + 4)s^{\beta} \exp\left\{i\pi(1 - \beta)/2\right\}\right] \tag{5.33}$$

where

$$\alpha = 1 + (0.5)t, \tag{5.34}$$

$$\beta = (0.5) + (0.5)u. \tag{5.35}$$

(3) Pure Resonance,

$$F_3(s,t) = G\left[\frac{(A - s) + i\Gamma}{(s - A)^2 + \Gamma^2}\right] P_\ell(\cos\Theta) . \tag{5.36}$$

The particle masses are taken to be unity.

(4),(5) Interference Models,

$$F_4 = F_1 + F_3, \tag{5.37}$$

$$F_5 = F_2 + F_4. \tag{5.38}$$

These models have been studied for several values of the parameters, and we believe it may be important to study how interference effects change as functions of the coupling strength, in order to understand bootstrap problems. However, for economy in space, we give only two diagrams to indicate interference patterns, and briefly describe other variations.

The phase contours for a pure Regge background of type F_1 have been illustrated in Section 3. The oscillations will be enhanced near the zeros of the residue factors. The general features of F_2 are similar to those of F_1, except for a displacement of the "symmetry" of the phase contours towards the direction of backward scattering.

The phase contours for S-state interference are illustrated in Figure (5.6) using the following parameters:

$$F_4; \quad G = 10, \quad A = 3, \quad \ell = 0, \quad \Gamma = 0.2. \tag{5.39}$$

The fixed complex pole, at $s = 3 + (0.2)i$, leads to a bunching of the phase contours near $s = 3$ as suggested from our earlier discussion in this section.

The interference model F_4 for a P-state resonance leads to a single zero that may be complex. We have illustrated this model in Figure 5.7 for parameters that give a real zero,

$$G = 10, \quad A = 3, \quad \ell = 1, \quad \Gamma = 0.2. \tag{5.40}$$

It will be noted that only in the forward direction do we get the phase change through 90 deg. (as s increases) that might be expected for a dominant resonance. This is because the background also has a phase that is not too different from 90 deg. In the near-backward direction the resonance gives a phase of -90 deg. and tends to cancel with the background. The result is a rather rapid change of phase, and in this example there is a real zero of the amplitude. In Section 7 we will see similar effects for pion nucleon scattering amplitudes obtained by phase shift analysis.

6. REGGEIZED RESONANCE TERMS

One of the problems that must be solved in order to understand the relation between high energy and low energy behavior, is the manner in which zeros of the amplitude appear on the physical sheet as the momentum transfer is increased. In this section, we consider a model that throws some light on this problem, although it is unrealistic with regard to the singularities from which the zeros appear.

(a) Zeros of a Regge Term

In a Regge model, a scattering amplitude may be approximated, for large z, by

$$F(s,t) \sim b(s)P_{\alpha(s)}(z), \tag{6.1}$$

where, with equal mass particles,

$$z = 1 + \frac{2t}{s - 4m^2}. \tag{6.2}$$

When ℓ is an integer $P_\ell(z)$ has ℓ real zeros, all within the range $[-1,1]$. These zeros lead to the familiar high z behavior, z^ℓ. For ℓ real but not an integer, we consider

$$\ell = n + \epsilon, \qquad 0 < \epsilon < 1. \tag{6.3}$$

Near $z = -1$, with $z = x$ (real and $|x| < 1$),

$$P_\ell(x) \sim \frac{\sin \ell\pi}{\pi}\left[\log\left\{\frac{1}{2}(1 + x)\right\} + 2\gamma + 2\psi(\ell + 1)\right] + \cos(\ell\pi) \tag{6.4}$$

where γ and ψ denote Euler's constant and the ψ-function, respectively. When $(x + 1)$ is sufficiently small, the dominant term will be

$$\frac{\sin \ell\pi}{\pi} \log \frac{1}{2}(1 + x) \sim (-1)^n(\ell - n) \log \frac{1}{2}(1 + x). \tag{6.5}$$

Thus, as ℓ changes from n to $n + \epsilon$, $P_\ell(x)$ will change from $(-1)^n$ to

$$(-1)^{n+1}\epsilon\left|\log \frac{1}{2}(1 + x)\right|. \tag{6.6}$$

A new zero develops in $(-1 < z < 1)$ when $\epsilon > 0$, which is not present when $\epsilon < 0$. As $\epsilon \to 0$ the zero will tend to -1. The zeros of $P_\ell(z)$, are shown in Figure 6.1(a) for ℓ real. The corresponding zeros of $F(s,t)$, given by (6.1), are shown in Figure 6.1(b), when $\alpha(s)$ increases through real values. In Regge theory with bosons, it is reasonable to assume $\alpha(s)$ to be real for s below threshold. However, above threshold $\alpha(s)$ will be complex. We will discuss the effects of this on phase contours at the end of this section. The zeros will still emerge from $z = -1$, but will then become complex.

(b) A Symmetrized Regge Model

Before considering phase contours for a Regge model, we will note the location of zeros when the model is first symmetrized to give even signature, and then a non-zero background is introduced. The even signature form will be

$$F(s,z) = -\left[b(s)\, P_{\alpha(s)}(z) + b(s)\, P_{\alpha(s)}(-z)\right]\left\{\cos\left(\frac{1}{2}\alpha\pi\right)\right\}^{-1}. \tag{6.7}$$

This has an asymptotic phase, for real positive $z = x + i0$,

$$\phi(s, x + i0) \sim \pi - \frac{1}{2}\pi\alpha(s), \tag{6.8}$$

which is characteristic of an even signature amplitude. This amplitude remains finite when α equals an odd integer, except at isolated zeros in the z plane, and it does not have a pole when α is even. It is not a relevant model when α is less than zero, and will not be considered for such values. We initially consider only real values of $\alpha(s)$, even though s should be above threshold when $\alpha > 2$.

The zeros $z_0(s)$ of the amplitude are shown in Figure 6.2(a) for real z, as a function of $\alpha(s)$.

When there is a complex background, the zeros will become complex. In Figure 6.2(b) we show the trajectories of the two leading pairs of zeros in the complex z plane, as s varies. One pair of zeros starts from $z = \pm 1$ when $\alpha(s) = 0$, and the second pair starts

from $z = \pm 1$ when $\alpha(s) = 2$. They are taken to be symmetric in relation to $z = 0$ by analogy with Figure 5.1. However, with a background that depends on t one would not have this symmetry.

(c) Phase Contours for the Symmetrized Model

It is useful to consider phase contours in the complex z plane and see how they vary for increasing $\alpha(s)$, and relate them to contours in the real (s,t) plane. We note again that, when there are zeros present, the labeling of phase contours becomes ambiguous. This difficulty could be removed by forming suitable integrals so as to construct univalent functions. However, we believe that information (about zeros in particular) would be lost in a formalism based on univalent functions, and a new construction would be needed each time new zeros appeared. In spite of this, it is very probable that univalent functions would be required for rigorous developments of our heuristic approach. This would require an extension of the work of Khuri and Kinoshita on forward amplitudes.[11]

Phase contours are shown in the z plane, for three values of $\alpha(s)$, in Figure 6.3(a), (b), and (c). It should be noted that the zeros emerge from the singular points (branch points at $+1$ and -1), bringing the phase contours with them. We would expect that this feature may occur only for an amplitude that diverges at the singular points, since otherwise any emerging zero would be swamped (i.e. displaced) by the background. In Figure 6.3(a) the contours $\phi = \pi$ should

be regarded as dividing at the real axis so that $(\pi - \epsilon)$ goes through the first zero on the right, and $(\pi + \epsilon)$ goes through the first zero on the left. Phase contours for intermediate values of ϕ are similarly distorted so that they cross the real axis only by going through one of the zeros of the amplitude (marked with X in Figure 6.3).

In Figure 6.4, we show the corresponding phase contours in the real (s,t) plane. The labeling of these contours uses the same prescription as in Figure 6.3, so that the phase is continuous through asymptotic values in the t plane. Equivalently, one could circle below all zeros in the real (s, t) plane of Figure 6.4, keeping $t + i0$ above the t and u branch cuts in the t plane.

(d) Phase Contours and Complex Regge Trajectories

When a Regge pole is continued above threshold, the trajectory becomes complex

$$\alpha(s) = \alpha_1 + i\alpha_2. \tag{6.9}$$

The corresponding Regge term in the amplitude for large t is given by

$$\frac{b(s)\, t^{\alpha} \exp\left[i\pi\left(1 - \frac{1}{2}\alpha\right)\right]}{\sin\left[\frac{1}{2}\alpha\pi\right]\ \Gamma(1 + \alpha)}. \tag{6.10}$$

When α is complex there are two new features to consider. The first arises from the effects on the phase from the resonance poles that

correspond to zeros of $\sin\left(\frac{1}{2}\alpha\pi\right)$. If our continuation in s is above the threshold branch cut, these resonance poles will be in the lower half of the second sheet of the s plane, at points where $\alpha(s)$ is an even integer. This important feature will be considered in detail in the next paper, when we discuss crossing symmetry and phase contours.

The second new feature, that arises when α is complex, comes from the exponent of t in (6.10). This gives a contribution to the phase equal to

$$\alpha_2(s) \log (t/t_0), \tag{6.11}$$

where t_0 provides an arbitrary normalization. As t tends to infinity, all phase contours will be dominated by this term, so they will all tend asymptotically to $s = 4m^2$, where $\alpha_2(s)$ becomes zero. For fixed s, there will be a logarithmic oscillation in the phase. This is a slow variation compared with oscillations that arise from interference between terms involving different powers of t. It may, therefore, be unimportant to some aspects of the study of phase contours.

7. LOW ENERGY SOLUTIONS FOR PION NUCLEON PHASE CONTOURS

(a) Formulae and Kinematics

It is not clear which amplitudes are most suitable for showing the phase properties for any particular collision process. There is a conflict between the requirements for simplicity at high energy, where exchanged Regge poles are assumed to dominate, and at low energy, where isospin amplitudes in the direct channel are more simple. We have given preference to high energy t-channel exchange processes. For u-channel exchange, the isospins are mixed. We study the phase contours for the following amplitudes for pion-nucleon scattering,

$$A'^{(+)}, \quad B^{(+)}, \quad A'^{(-)}, \quad B^{(-)}, \tag{7.1}$$

where

$$A' = A + \left[\frac{E_L + t/4M}{1 - t/4M^2}\right], \tag{7.2}$$

E_L = pion lab. energy, and

$$A'^{(+)} = \frac{1}{2}\left[A'(\pi^- p) + A'(\pi^+ p)\right], \tag{7.3}$$

$$A'^{(-)} = \frac{1}{2}\left[A'(\pi^- p) - A'(\pi^+ p)\right]. \tag{7.4}$$

$B^{(+)}$ and $B^{(-)}$ are given by similar relations. Thus

$$A'^{(cex)} = -\sqrt{2}\ A'^{(-)}, \tag{7.5}$$

$$B^{(cex)} = -\sqrt{2}\ B^{(-)}. \tag{7.6}$$

The relation of these invariant amplitudes to the partial wave helicity amplitudes are given by Chew and Jacob[15] and by Eden.[1] The related experimental quantities are,

$$\frac{d\sigma}{dt} = c\left[K_a|A'|^2 + K_b|B|^2\right], \tag{7.7}$$

$$P = \frac{-2\ \mathrm{Im}\ B^*A'(K_aK_b)^{\frac{1}{2}}}{K_a|A'|^2 + K_b|B|^2}, \tag{7.8}$$

where

$$K_a = 1 - t/4M^2, \tag{7.9}$$

$$K_b = -\frac{t}{4M^2}\left[\frac{(M + E_L)^2}{1 - t/4M^2} - s\right], \tag{7.10}$$

$$c = \frac{(0.226M)^2}{q_s^{\ 2}s}, \tag{7.11}$$

$$s = M^2 + \mu^2 + 2ME_L , \tag{7.12}$$

$$q_s^{\,2} = (\text{c.m. momentum})^2. \tag{7.13}$$

(b) Experimentally Determined Phase Contours

The most recent analyses of partial wave phase shifts from pion nucleon experiments are those of Lovelace,[16] Bareyre[17] and Johnson.[18] In and near the physical scattering region the phase and modulus of each of our invariant amplitudes can be computed from each of the phase shift solutions. We will illustrate the results in this section by selecting certain phase and modulus contours. At this stage we are concerned only with the form of the "experimental" amplitudes given by the phase shift solutions. For these, the phase contours provide: (i) an illustration of characteristic features such as zeros of the amplitude that were discussed earlier, (ii) a method for comparing different solutions for the same amplitude, and (iii) a means for noting "difficult" energies, where rapid phase changes may indicate an incorrectly continued solution, or may indicate a genuine experimental complexity.

At a later stage it is hoped that background and resonance contributions can be sufficiently well understood to permit a solution of the problem of joining high energy and low energy solutions for scattering amplitudes. However, neither the data nor our knowledge of theory seems sufficient for this at present. We therefore give only a few phase contour diagrams to illustrate their general characteristics.

In Figures 7.1 and 7.2, respectively, we show the phase contours and the modulus contours derived from the Lovelace solutions to $A'^{(+)}$. We have used the kinetic energy of the pion T_π in the lab. system, instead of s, the invariant $(\text{energy})^2$, as the former is more commonly used in experimental work. They are related by

$$s = (M + \mu)^2 + 2MT_\pi . \tag{7.14}$$

Several aspects of the phase contour diagram, Figure 7.1, appear to be significant:

(i) The resonances that show most conspicuously are those at $T_\pi = 0.19$ (the 1238 resonance) and the resonances near $T_\pi = 0.9$ (1670, D_{15}; 1688, F_{15}; and 1700, S_{11}). The effect of the latter is most noticeable below the resonance value, since the background phase in this region is about 100 deg. Above resonance, near t = 0, the background and resonance contributions are nearly in phase. Below the resonance its phase falls below 90 deg, and this brings the phase of the full amplitude down to 90 deg as indicated. The 1238 resonance is sufficiently dominant to give both a phase of 90 deg near the forward direction and minus 90 deg near the backward direction

(ii) There is a concentration of phase contours along a scattering angle between 90 deg and 120 deg over the considerable energy range, $T_\pi = 0.1$ to 0.6 GeV. This corresponds to a valley in the modulus contour diagram, Figure 7.2. As expected from our earlier discussion,

a small modulus permits (perhaps causes) rapid changes of phase of the scattering amplitude.

(iii) There are two real zeros of the scattering amplitude $A'^{(+)}$ in the physical region, namely the points where the phase contours cross at $(T_\pi, -t)$ equals (0.34, 0.27) and (1.26, 0.91). The first of these is clearly in the region dominated by resonances, and it can be regarded as a result of resonance interference. The second one occurs at a higher energy, and may perhaps be more readily attributed to background interference of forward and backward Regge terms. Both zeros occur within regions where the modulus of the amplitude is seen to be small in Figure 7.2.

(iv) From forward scattering $(t = 0)$ out to nearly 90 deg angle of scattering, there is a phase plateau for $A'^{(+)}$ in the second quadrant, mostly with the phase between 100 deg and 150 deg. It is interesting that Regge exchange gives a similar phase for $A'^{(+)}$, as we shall see in more detail in Section 8. This indicates that the deviations that resonances cause from Regge background are remarkably small for this amplitude (possibly indicating a bootstrap effect).

For comparison with Figure 7.1, which was derived from the Lovelace[16] phase shifts for $A'^{(+)}$, we give in Figure 7.3 the phase contours for $A'^{(+)}$ that are obtained from a preliminary set of phase shifts given by Johnson.[18] It should be noted that our phase contour diagrams provide a more sensitive comparison between phase shift solutions than is justified by the experimental evidence, especially

where the modulus of the scattering amplitude is small. Below $T_\pi = 0.45$ the Lovelace phase shifts were used. The comparison of the Johnson results that give Figure 7.3 and those of Lovelace (Figure 7.1), should be made only above $T_\pi = 0.45$ GeV. There is a very satisfactory resemblance between Figure 7.1 and Figure 7.3. The most notable difference is that the zero of $A'^{(+)}$ at (.126, 0.91) in Figure 7.1 is not present in Figure 7.3. It seems that the latter corresponds to two complex zeros near the point (1.35,1.00). For consistency one would therefore expect a second real zero at a higher energy if the Lovelace solutions were continued up to $T_\pi = 1.6$.

The phase contours from the Loevlace phase shifts for $B^{(+)}$, $A'^{(-)}$ and $B^{(-)}$ are shown in Figures 7.4, 7.5 and 7.6. They are obviously much more complicated that those for $A'^{(+)}$, and they are instructive in two respects. Firstly, they indicate regions, or energy bands, of great complexity, that involve rapid changes of phase and should be verified by further experiment. This is particularly evident in the energy region

$$0.80 < T_\pi < 0.90. \tag{7.15}$$

This lies just below the three resonances (1670, 1680,1700) and has earlier been noted by Lovelace as a region where further experimental evidence is desirable.

The second application of phase contour diagrams lies in the search for continuity between phase shift solutions. Rapid changes of phase can be expected when the modulus of an amplitude is very small, but they are unlikely if it is large. In the latter case there would be dramatic changes in polarization that could be observed.

Other applications of these phase contours include using them as a means of searching for complex zeros. The significance of complex zeros will be considered in the next paper.

8. HIGH ENERGY SOLUTIONS FOR PION-NUCLEON PHASE CONTOURS

We hope eventually to find a self-consistent topology for phase contours that will assist in establishing a method for connecting high energy and low energy approximations for studying scattering amplitudes. At this stage, however, we are concerned primarily with finding out what phase contours look like, and how their main features can be interpreted. At high energy there are no model independent methods for determining phase contours from experiment. The nearest approach to phenomenology is given by the Regge solutions for near-forward, and for near-backward, scattering. Up to now the experimental data in forward and backward directions has been fitted almost independently. In order to study their relation to each other by means of phase contours we require an analytic function that goes over to the forward and backward Regge solutions in the appropriate regions. This can be obtained simply by adding the two solutions. We consider this procedure as a means of obtaining a first approximation to the correct topology of the actual phase contours.

The sum of these Regge solutions is a valid approximation within the Regge phenomenological assumptions, at high energies near the forward and backward directions. We will extrapolate in two ways. Firstly to large angles at high energies. This requires specific assumptions that cannot at this stage be based on any experimental evidence. We assume (i) that the leading poles continue to dominate at large angles, and (ii) that the trajectories continue to fall as t decreases. The first

assumption probably does not affect the topology (as opposed to the spacing) at large angles and high energies. The second assumption affects their topology as was discussed earlier in Section 3.

Our second extrapolation of the sum of Regge solutions is to energies below those at which Regge approximations are reasonable. Our purpose here is to obtain the Regge "background" at low energies in a moderately realistic example, and also to study its phase contours and see whether there are any striking interference effects between the forward and backward Regge solutions, when their magnitudes are comparable.

Our detailed assumptions and choice of Regge solutions will be described in the next paragraph and in the Appendix.

(a) The Regge Solutions Used

We use a modified form of one of the Regge solutions for forward scattering, that have been shown to fit pion-nucleon high energy data by Rarita, Riddell, Chiu and Phillips,[19] (denoted RRCP in the following). Their original solutions, on which ours are based, are given below. Our modifications are chosen to introduce zeros in the residue functions when the trajectory goes through a negative integer of appropriate signature. They are

(i) For P and P′ exchange contributions, when $\alpha < -1$, $[\alpha = \alpha_P(t)$ or $\alpha_{P'}(t)]$,

$$A(\text{modified}) = \sin\left(\frac{\pi\alpha}{2}\right) A(\text{original}). \tag{8.1}$$

(ii) For ρ exchange contributions, when $\alpha_\rho < -2$,

$$A(\text{modified}) = -\cos\left(\frac{\pi\alpha}{2}\right) A(\text{original}). \tag{8.2}$$

In the backward direction, our amplitudes are modified from those of Chiu and Stack[20] (discussed and tabulated in the Appendix). The modification to permit extrapolation without unphysical pole contributions is,

(iii) For N and Δ exchange amplitudes, when $\alpha < -2$, $[\alpha = \alpha_N(u),$ or $\alpha_\Delta(u)]$,

$$A(\text{modified}) = \frac{\sin\left[\frac{1}{2}\pi\left(\alpha - \frac{1}{2}\right)\right] A(\text{original})}{\sin\left[\frac{1}{2}\pi\left(\alpha_2 - \frac{1}{2}\right)\right]} \tag{8.3}$$

where $\alpha_2 = -2 + i\mathrm{Im}\,\alpha$ Similar modifications are introduced in the B amplitudes. There are some complications in evaluating the phase of the backward Regge amplitude due to the fact that the trajectory $\alpha(u)$ contains a term involving $(u)^{\frac{1}{2}}$. These complications are discussed in the Appendix, where these amplitudes are given.

The forward amplitudes that we modify, are those called solution 1 by RRCP. The formulae for these amplitudes are;

$$A' = C_0 \exp(C_1 t)\, \alpha(\alpha + 1)\xi(E_L/E_0)^\alpha, \quad \text{for } P \text{ and } P', \tag{8.4}$$

$$A' = C_0\left[(1 + C_2)\exp(C_1 t) - C_2\right](\alpha + 1)\xi(E_L/E_0)^\alpha, \quad \text{for } \rho \tag{8.5}$$

$$B = D_0 \exp(D_1 t)\alpha^2(\alpha + 1)\xi(E_L/E_0)^{\alpha-1}, \quad \text{for } P \text{ and } P', \tag{8.6}$$

$$B = D_0 \exp(D_1 t)\alpha(\alpha + 1)\xi(E_L/E_0)^{\alpha-1}, \quad \text{for } \rho, \tag{8.7}$$

where

$$\xi(t) = \frac{\exp\left[i\left(\pi - \frac{1}{2}\pi\alpha\right)\right]}{\sin\frac{1}{2}\pi\alpha} \quad \text{for } P \text{ and } P', \tag{8.8}$$

$$\xi(t) = \frac{\exp\left[i\left(\frac{1}{2}\pi - \frac{1}{2}\pi\alpha\right)\right]}{\cos\frac{1}{2}\pi\alpha} \quad \text{for } \rho, \tag{8.9}$$

and

$$\alpha(t) = \alpha(0) + t\alpha'. \tag{8.10}$$

The symbol E_L denotes the pion energy in the lab. system, and E_0 denotes a scale factor, which is taken to be 1 GeV.

The following values are chosen for the parameters, (RRCP solution 1),

	$\alpha(0)$	α' $(GeV)^{-2}$	C_0 (mb GeV)	C_1 $(GeV)^{-2}$	D_0/C_0 $(GeV)^{-1}$	D_1-C_1 $(GeV)^{-2}$
P	1.0	0.12	7.23	2.36	-3.69	7.02
P′	0.73	1.50	16.35	0.44	-3.52	3.42

	$\alpha(0)$	α'	C_0	C_1	C_2	D_0(mb)	D_1
ρ	0.58	0.94	1.47	0.20	15.2	26.3	0.34

(b) Phase Contours From Regge Solutions

We have drawn the phase contour diagrams for the A' and B amplitudes given by the sum of the forward and backward Regge solutions. These solutions were chosen to fit experimental pion-nucleon results in the following regions:

Forward solution (RRCP 1)[19]

$$5.9 \leqslant T_\pi \leqslant 25 \text{ GeV}.$$

$$0 \leqslant -t \leqslant 1 \ (\text{GeV}/c)^2.$$

Backward solution (Chiu and Stack)[20]

$$4 \leqslant T_\pi \leqslant 10 \text{ GeV}$$

$$-u \leqslant 1(\text{GeV}/c)^2.$$

Our extrapolated solutions were evaluated in the whole of the physical region for pion nucleon scattering, for energies in the range

$$1 \leqslant T_\pi \leqslant 7 \text{ GeV}.$$

The resulting phase contour diagrams are shown in Figure 8.1, $A'^{(+)}$; Figure 8.2, $B^{(+)}$; Figure 8.3, $A'^{(-)}$; Figure 8.4, $B^{(-)}$. We have labeled the phases in the range

$$-180 \text{ deg} < \phi(s,t) \leqslant 180 \text{ deg}.$$

This avoids the difficulty of specifying a path by which each phase is to be evaluated, so as to prevent ambiguities from the zeros of the amplitudes.

It will be seen that the pion nucleon phase contours have the characteristic topology, that was suggested by our simpler Regge model in Section 3, provided the pion energy exceeds about 4 GeV. However, at lower energies there are striking interference phenomena between the forward and backward Regge terms.

At the highest energies shown, the high densities of phase contours at certain values of s, and of t, arise from the zeros in the residues of the leading terms in each amplitude. Thus in Figure 8.4, the zero of the factor $\alpha_\rho(t)$ in $B^{(-)}$, leads to a rapid change of phase near $t = -0.6$. At $\alpha_\rho(t) = 0$, the ρ contribution has a pure imaginary phase factor (8.9). Thus $\text{Im}B^{(-)}$ will have a single zero while $\text{Re}B^{(-)}$ will have a double zero as $s \to \infty$. This gives a

rapid phase increase through 180 deg near the zero. At lower energies, the interference from poles exchanged in the u-channel, leads to a sequence of real zeros of $B^{(-)}$ in the physical region.

The effect of the zero in the P' contribution is somewhat different. This contribution appears in $B^{(+)}$ [and also $A'^{(+)}$]. At the zero of $\alpha_{P'}$, there is a double zero of Im[P' term] and a single zero of Re[P' term]. Combining this with the P contribution, one finds a minimum in the phase of $B^{(+)}$. This minimum is indicated by the -120 deg contour in Figure 8.2. It will be recalled that near the forward direction, only P and P' contribute to $B^{(+)}$.

The most striking effect of interference is the occurence of zeros if all four amplitudes in the physical region for pion nucleon scattering. None of them can be identified with the zeros at low energy that were indicated by the phase contour described in Section 7. We do not know how to combine resonances with a Regge background in a realistic way without double counting. Presumably resonances can be expected to move these zeros, possibly to an unphysical sheet. However, some of them are at sufficiently high energy that the effects of resonances should be small. These zeros are closely related to the occurrence of zeros in the residue factors, which lead to a sharp change in the interference between different Regge terms. When such zeros occur in the residue that corresponds to the leading trajectory, they lead to a condensation of phase lines (-90 deg $< \phi <$ 90 deg) as the energy becomes asymptotic.

Although the phases of the Regge solutions at low energy do not in general correspond at all closely to the "experimental" values of the phase obtained from the phase shift solutions in Section 7, there is one interesting exception. This is the $A'^{(+)}$ amplitude in the near forward direction

$$0 < (-t) < 0.5 (\mathrm{GeV}/c)^2 .$$

In this range the Regge phase agrees quite well with the phase shift solution Figure 7.1, down to $T_\pi = 1.06$ GeV. We have plotted the modulus contours for $A'^{(+)}$ in Figure 8.5. This should be compared with the modulus contours from the phase shift solutions shown in Figure 7.2. There is remarkable good agreement down to $T_\pi = 1.0$ GeV. It is evident however that more subtle approximations will be required to obtain even qualitative agreement for the other amplitudes.

9. DISCUSSION

In this paper our study of the properties of phases of scattering amplitudes has indicated a number of applications, particularly of the method of phase contours. The applications that we regard as most promising include:

(1) The use of phase contours for the interpretation of experiments. We have noted their value for pion-nucleon scattering up to 1.4 Gev in Section 7, particularly when combined with modulus contours. Their functions include: the provision of an instructive visual comparison of different phase shift solutions; their use for indicating doubtful continuation of solutions from one energy to the next, and their use for indicating regions where the amplitude is so complicated that more detailed experiments are required.

(2) The use of phase contours (and modulus contours) as a guide in developing a phenomenological theory that includes both the low and medium energy resonance regions and the high energy (Regge) regions. We have touched on this problem in Sections 7 and 8, but at this stage we have not attempted to combine resonances and Regge theory in a realistic model; our models discussed in Section 5 were designed only to give a preliminary orientation on phase contours for resonances plus a Regge background.

(3) Crossing symmetry in one variable is implicit in Regge theory. It appears that phase contours provide a method for studying crossing symmetry in s, t and u variables. They lead to consistency

requirements between high energy behavior and the location of zeros of scattering amplitudes, and give rather a clear indication of some effects of varying coupling parameters, such as scattering lengths. Some preliminary aspects of this problem were considered in Section 6, and it will be developed further in the next paper of this series.[22]

(4) Phase contours, and the associated complex surfaces on which the phase of a scattering amplitude is constant, together with curves and surfaces of zeros, provide a method for specifying high energy behavior that is useful in the context of Regge theory and may also be used in generalizing that theory. This should permit one to specify conditions that show how asymptotic behavior at fixed momentum transfer may be related to fixed angle behavior. This will be discussed in a later paper.

ACKNOWLEDGMENT

We are indebted for hospitality and for helpful discussions to Professor G. F. Chew at the Lawrence Radiation Laboratory, Berkeley, and to Dr. L. Van Hove at CERN, Geneva.

APPENDIX

Complications in Evaluating the Phase of the Backward Regge Amplitude Due to $\frac{d\alpha}{dw} = 0$

Define the invariant amplitudes in the u-channel to be

$$A^u = 4\pi\left(\frac{W_u + M}{E_u + M} f_1^u - \frac{W_u - M}{E_u - M} f_2^u\right)$$

$$B^u = 4\pi\left(\frac{f_1^u}{E_u + M} + \frac{f_2^u}{E_u - M}\right) \qquad A(1)$$

The Regge asymptotic behavior is given by (see for example Singh[21])

$$f_1^u \xrightarrow[s\to\infty]{} \frac{E_u + M}{\sqrt{u}} \beta^+ s^{\alpha^+ - \frac{1}{2}} \xi^+$$

u fixed

$$f_2^u \xrightarrow[s\to\infty]{} -\frac{(E_u - M)}{\sqrt{u}} \beta^- s^{\alpha^- - \frac{1}{2}} \xi^- \qquad A(2)$$

u fixed

with $\pm$ indicating the $\pm\sqrt{u}$ argument. $\xi = -\dfrac{1 \pm e^{-i\pi(\alpha - \frac{1}{2})}}{\sin\frac{\pi}{2}(\alpha - \frac{1}{2})}$.

The β defined in this way is the same as the β in Chiu and Stack.[20] The phases of A^u, B^u, and by crossing also A^s, B^s and hence A^s and B^s can be evaluated through (1) and (2).

To illustrate the complication, we will evaluate the corrections explicitly near $u = 0$ for the nucleon amplitude. Following Chiu and Stack,

$$\alpha_N = \alpha_0 + \alpha_1\sqrt{u} + \alpha_2 u \,, \qquad A(3)$$

$$\beta = \left(\alpha + \frac{1}{2}\right)\left(\alpha + \frac{3}{2}\right)\left(\sqrt{u} - \sqrt{u_0}\right) D \exp\left[a\sqrt{u} + bu\right].$$

Expanding f_1 and f_2 in $\sqrt{u}$, one obtains

$$f_1{}^u \longrightarrow \frac{E_u + M}{\sqrt{u}} \text{const}\left(1 + C_1\sqrt{u}\right)\left[\frac{\exp\left\{-\frac{i\pi\left(d_0 - \frac{1}{2}\right)}{2}\right\}}{\sin\left\{\frac{\pi}{2}\left(d_0 - \frac{1}{2}\right)\right\}}\left(d_0 + \frac{1}{2}\right)\left(d_0 + \frac{3}{2}\right)\right]$$

$$f_2{}^u \longrightarrow -\frac{\left(E_u - M\right)}{\sqrt{u}} \text{const}\left(1 - C_1\sqrt{u}\right)\left[\frac{\exp\left\{-\frac{i\pi\left(d_0 - \frac{1}{2}\right)}{2}\right\}}{\sin\left\{\frac{\pi}{2}\left(d_0 - \frac{1}{2}\right)\right\}}\left(d_0 + \frac{1}{2}\right)\left(d_0 + \frac{3}{2}\right)\right] \qquad A(4)$$

where

$$C_1 = \bar{f}_1 \frac{d}{d\sqrt{u}}\left(\ln \bar{f}_1\right)\Big|_{\sqrt{u}\ z0} \,, \qquad \bar{f}_1 = \frac{\sqrt{u}}{E_u + M} f_1 . \qquad A(5)$$

Substituting (3) and (4) in (5) one obtains

$$C_1 = \frac{1}{\sqrt{u_0}} + a + \frac{\alpha'}{\alpha_0 + \frac{1}{2}} + \frac{\alpha'}{\alpha_0 + \frac{3}{2}} - \frac{i\pi\alpha'}{2} + \frac{\frac{\alpha'\pi}{2}\cos\left\{\left(\alpha_0 - \frac{1}{2}\right)\frac{\pi}{2}\right\}}{\sin^2\left\{\frac{\pi}{2}\left(\alpha_0 - \frac{1}{2}\right)\right\}} + \alpha' \ln s \qquad A(6)$$

Now let us look at a specific example: for the phase contours included, the backward amplitudes have the following parameters -

$$\begin{cases} \alpha_N = -0.325 + 0.118\sqrt{u} + 1.061\, u\,, \\ \beta_N = \left(\sqrt{u} - \sqrt{u_0}\right) 249.9 \exp[-0.608\sqrt{u} - 0.217\, u] \cdot \left(\alpha + \frac{1}{2}\right)\left(A + \frac{3}{2}\right) \end{cases} \qquad A(7)$$

with $\sqrt{u_0} \sim 0.85$. For completion, the Δ parameters are:

$$\alpha_\Delta = -0.100 + 0.248\sqrt{u} + 0.844\, u\,,$$

$$\beta_\Delta = 8.830 \exp[0.178\sqrt{u} + 1.073\, u]. \qquad A(8)$$

At $T_\pi = 20$ GeV, or $s = 41$ GeV^2, one has

$$C_1 = (0.055) - i(0.185)\,. \qquad A(9)$$

From (4), (1) and (2) one has near $u = 0$,

$$A^u \sim \text{const}(1 + C_1 M)\left[\frac{\exp\left[-\frac{i\pi}{2}\left(\alpha_0 - \frac{1}{2}\right)\right]}{\sin\left\{\frac{\pi}{2}\left(\alpha_0 - \frac{1}{2}\right)\right\}}\left(\alpha_0 + \frac{1}{2}\right)\left(\alpha_0 + \frac{3}{2}\right)\right],$$

$$B^u \sim \text{const}\, C_1\left[\frac{\exp\left[-\frac{i\pi}{2}\left(\alpha_0 - \frac{1}{2}\right)\right]}{\sin\left\{\frac{\pi}{2}\left(\alpha_0 - \frac{1}{2}\right)\right\}}\left(\alpha_0 + \frac{1}{2}\right)\left(\alpha_0 + \frac{3}{2}\right)\right]. \qquad A(10)$$

Hence the phase correction for A^u is: (from (10))

$$\begin{cases} \theta_c^{\ A} \sim tg^{-1}\left[\dfrac{-0.185M}{1 - 0.55M}\right] \sim -20 \text{ deg}, \\ \theta_c^{\ B} \sim tg^{-1}\left[\dfrac{0.185}{0.55}\right] \sim +20 \text{ deg}, \end{cases}$$

here the overall signs are ignored. Of course in the limit $s \to \infty$, eq.(6) implies C_1 will eventually approach a real value. But e.g. for $\dfrac{ReC_1}{ImC_1} = 10$, one would need $ReC_1 = 1.85 \Rightarrow \alpha' \ln\left(\dfrac{s_2}{s_1}\right) = 1.85 + 0.55$, where we have picked $s_1 = 41$. This gives

$$s_2 = \left[\exp(20.3)\right] s_1 \text{ GeV}^2 = 7 \times 10^8 s_1 \text{GeV}^2,$$

$$\text{or } T_\pi = 1.4 \times 10^9 \text{GeV}.$$

However, the situation might not be as bad, if α' is very small, then from (6) one sees θ_c could be small. At present the parameter α' is not very well determined from experiment.

The phase for our solution is also complicated due to the presence of Δ contribution. Unfortunately we have α_Δ slightly higher than α_N. So at super high energy, Δ will dominate over the nucleon contribution.

FOOTNOTES AND REFERENCES

* This work was done under the auspices of the United States Atomic Energy Commission.

† The Cavendish Laboratory, Cambridge, England, after January 1, 1968.

1. R. J. Eden, High Energy Collisions of Elementary Particles, (Cambridge University Press, New York, 1967).
2. R. Dolen, D. Horn and C. Schmid, Phys. Rev. Letters 19, 402 (1967).
3. A. V. Stirling and C. B. Chiu, CERN preprint (1967).
4. Y. S. Jin and A. Martin, Phys. Rev. 135, B1369, (1964).
5. M. Sugawara and A. Tubis, Phys. Rev. 130, 2127 (1963).
6. T. Kinoshita, Phys. Rev. 154, 1438 (1967).
7. R. J. Eden and L. Łukaszuk, Nuovo Cimento 47, 817 (1967).
8. N. N. Meimann, Soviet Physics JETP 16, 1609 (1963).
9. A. A. Logunov, Nguyen van Thien, I. T. Todorov, and O. A. Krustalev, Phys. Rev. Letters 7, 69 (1963).
10. L. Van Hove, Rev. Mod. Phys. 36, 655 (1964).
11. N. N. Khuri and T. Kinoshita, Phys. Rev 140, B706 (1965).
12. Y. S. Jin and S. W. MacDowell, Phys. Rev. 138, B1279 (1965).
13. Y. S. Jin and A. Martin, Phys. Rev. 135, B1369 (1964).
14. S. Mandelstam, Nuovo Cimento 30, 1127, 1148 (1963).
15. G. F. Chew and M. Jacob, Strong Interaction Physics, (W. A. Benjamin, Inc., New York, 1963).
16. C. Lovelace, Report in the Berkeley Conference on High Energy Physics (1966).

17. P. Bareyre, C. Bricman and G. Villet, Saclay preprint (1967) (submitted to Phys. Rev.).

18. C. H. Johnson, Ph. D. Thesis, University of California, Berkeley (1967).

19. W. Rarita, R. J. Riddell, Jr., C. B. Chiu, and R. J. N. Phillips, Phys. Rev. (to be published) (1968).

20. C. B. Chiu and J. Stack, Phys. Rev. 153, 1575 (1967).

21. V. Singh, Phys. Rev. 129, 1889 (1963).

22. R. J. Eden and Chung-I Tan, "Phase Contours of Scattering Amplitudes II, Crossing Symmetry, Resonance Poles and High Energy Behavior", University of California, Lawrence Radiation Laboratory Report, UCRL-17922 (1967).

FIGURE CAPTIONS

Fig. 3.1. Phase contours in the real (s,t) plane for the simple Regge background given in Eq. (3.1). In this sketch the oscillations are larger than one finds in a more phenomenological model (see Fig. 8.1, for example).

Fig. 3.2. (a) The line $t = t_n$, in the real (s,t) plane, with two effective intersections, at s_1 and s_2, with $\mathrm{Im}F = 0$ contours.

(b) The amplitude F, as s varies from s_0 to infinity, along $t = t_n$ in Fig.(a).

(c)(d) The analagous diagrams to (a)(b), when there are also ineffective intersections with the $\mathrm{Im}F = 0$ contours.

Fig. 3.3. (a) Phase contours when the leading Regge trajectory has zero residue at t_1^0, t_2^0, t_3^0, $\cdots$.

(b) The behavior of F along the line s real, $t = t_1^0 + \epsilon$, from a finite point s_0 to infinity.

Fig. 3.4. (a) Phase contours in the real (s,t) plane when the Inequality (3.12) is satisfied.

(b) Phase contours when a fixed Pomeranchuk pole dominates at fixed angles.

Fig. 4.1. (a) The contours C_s and C_s in the complex s plane.

(b) An example of the mapping C_F of C_s on to the F plane.

(c)(d) Contours C_F that correspond to similar asymptotic behavior. C_F is the mapping of C_s in (a) but corresponds to a simpler contour than C_F in (b).

Fig. 4.2. (a) The phase contour $\phi(s,t) = n\pi$, giving $\mathrm{Im}F(s,t) = 0$, drawn in the real (s,t) plane.

(b) $\phi = n\pi$ in the complex s plane for $t = t_3$.

(c) $\phi = n\pi$ for $t = t_2$.

(d) $\phi = n\pi$ for $t = t_1$.

Fig. 4.3. (a) The phase contour $\phi(s,t) = n\pi$ in the real (s,t) plane.

(b) $\phi = n\pi$ for complex s, with t fixed just below the asymptotic value.

Fig. 4.4. (a) The curves C_s and C_s' in the s plane.

(b) The curves C_F and C_F' that correspond to C_s and C_s', when there is a complex zero of F at $s = s_0$.

Fig. 5.1. Phase contours in the complex $z = \cos\theta$ plane, for the D-state resonance model at resonance, (a) with $(B' - C) < 0$, and (b) with $(B' - C) > 0$. In both cases $B > 0$ and $B' > 0$.

Fig. 5.2. A solution for the phase contours for complex z, near a D-state resonance, showing two real zeros of the scattering amplitude $F(s,t)$.

Fig. 5.3. Illustrations of how curves of zeros $z = z_0(s,b)$ of $F(s,t)$, (formed by varying s through real values), can change from a situation having two real zeros to one having two complex zeros when the parameter b is varied.

Fig. 5.4. (a) The phase ϕ near a zero of F at (s_0,t_0), with $(s - s_0) = \mu(t - t_0)$. The complement phase ϕ is obtained when μ is constant but $(s - s_0)$ and $(t - t_0)$ change sign.

(b) Phase contours for real (s,t) near a zero of $F(s,t)$ with $\phi = \pi$ chosen as the discontinuity line where ϕ changes by $\pm 2\pi$.

Fig. 5.5. The drawings (a), (d) and (g) illustrate phase contours when there are two neighboring real zeros in the real (s,t) plane. Note that we interpret 180 deg and -180 deg as equivalent phase contours here. The figures (a), (b), (c) denote a variation of parameters for which the two zeros (a) become coincident (b) and then complex (c). Similar variations of parameters relate (d) to (e) and (f), and relate (g) to (h) and (i).

Fig. 5.6. Phase contours when there is S-state interference with a Regge background, from a resonance at $s = 3$. The phase values $\phi(s,t)$ are shown in degrees for the amplitude F_4 with $G = 10$, $A = 3$, $\ell = 0$ and $\Gamma = 0.2$.

Fig. 5.7. Phase contours for the model F_4 with $G = 10$, $A = 3$, $\ell = 1$, $\Gamma = 0.2$, showing P-state interference. Note that there is a zero of F where the phase lines cross.

Fig. 6.1. (a) Zeros of $P_\ell(z)$ for ℓ and z real.
(b) Zeros of $F(s,t)$ given by Eq. (6.1) when $\alpha(s)$ is real.

Fig. 6.2. (a) Zeros $z_0(s)$, shown as a function of $\alpha(s)$ for the Regge model Eq. (6.7) without background.
(b) Zeros $z_0(s)$ when the Regge model has a complex background. They are drawn in the z plane as $\alpha(s)$ increases.

Fig. 6.3. Phase contours, $\phi(s,z) = \text{constant}$, in the z plane for the symmetrized Regge model, Eq. (6.7), (a) when $0 < \alpha < 1$, (b) when $1 < \alpha < 2$, and (c) when $4 < \alpha < 5$. Note that contours (not drawn) for intermediate values of the phase would all be distorted near the real axis so that they go through an appropriate zero.

Fig. 6.4. Phase contours, in the real (s,t) plane, for a Regge model based on s-channel resonances, Eq. (6.7). For simplicity $\alpha(s)$ has been assumed to be real, and also to increase monotonically when s is above its threshold.

Fig. 7.1. Phase contours for $A'^{(+)}$ based on the (πp) phase shifts derived by Lovelace (1966).

Fig. 7.2. Modulus contours for $A'^{(+)}$ based on the (πp) phase shifts derived by Lovelace (1966).

Fig. 7.3. Phase contours for $A'^{(+)}$ based on preliminary (πp) phase shifts derived by Johnson (1967).

Fig. 7.4. Phase contours for $B^{(+)}$ (based on Lovelace phase shifts 1966).

Fig. 7.5. Phase contours for $A'^{(-)}$ (based on Lovelace phase shifts 1966).

Fig. 7.6. Phase contours for $B^{(-)}$ (based on Lovelace phase shifts 1966).

Fig. 8.1. Phase contours for $A'^{(+)}$ based on the superposition of forward and backward Regge solutions with extrapolation as described in the text.

Fig. 8.2. Phase contours for $B^{(+)}$ based on the superposition of forward and backward Regge solutions.

Fig. 8.3. Phase contours for $A'^{(-)}$ based on the superposition of forward and backward Regge solutions.

Fig. 8.4. Phase contours for $B^{(-)}$ based on the superposition of forward and backward Regge solutions.

Fig. 8.5. Modulus contours for $A'^{(+)}$ based on the superposition of forward and backward Regge solutions.

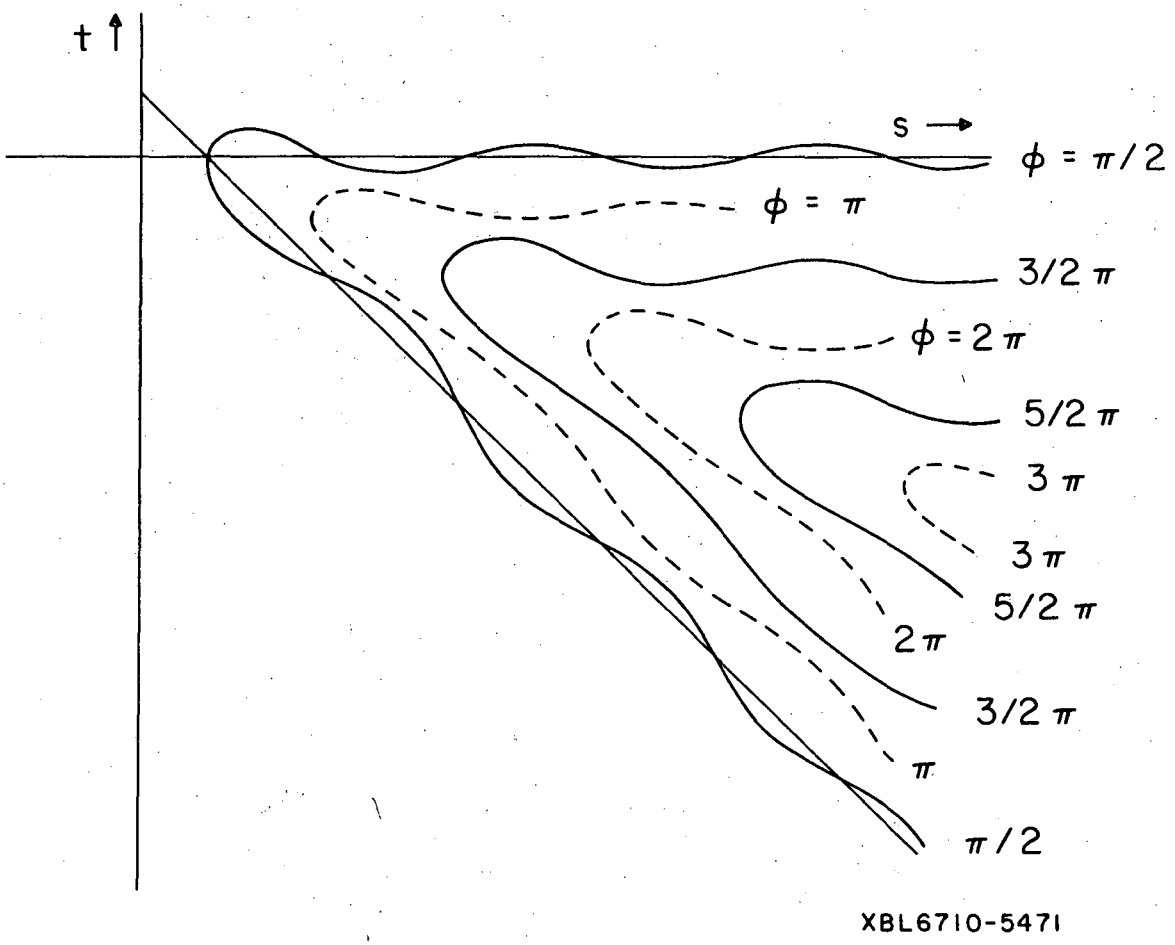
t
s
$\phi = \pi/2$
$\phi = \pi$
$3/2\,\pi$
$\phi = 2\pi$
$5/2\,\pi$
$3\,\pi$
$3\,\pi$
$5/2\,\pi$
2π
$3/2\,\pi$
π
$\pi/2$
XBL6710-5471

Fig. 3.1

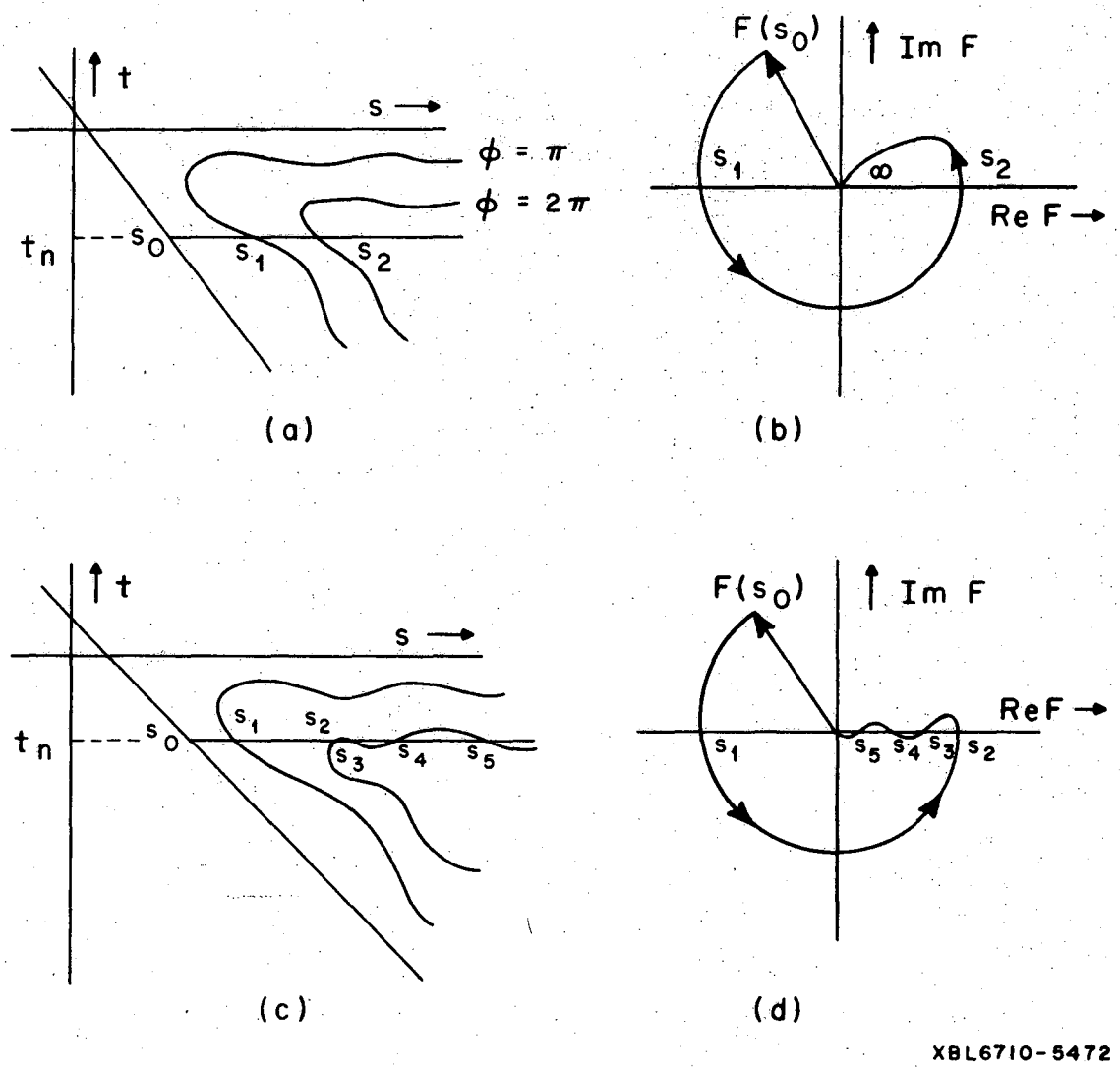

XBL6710-5472

Fig. 3.2

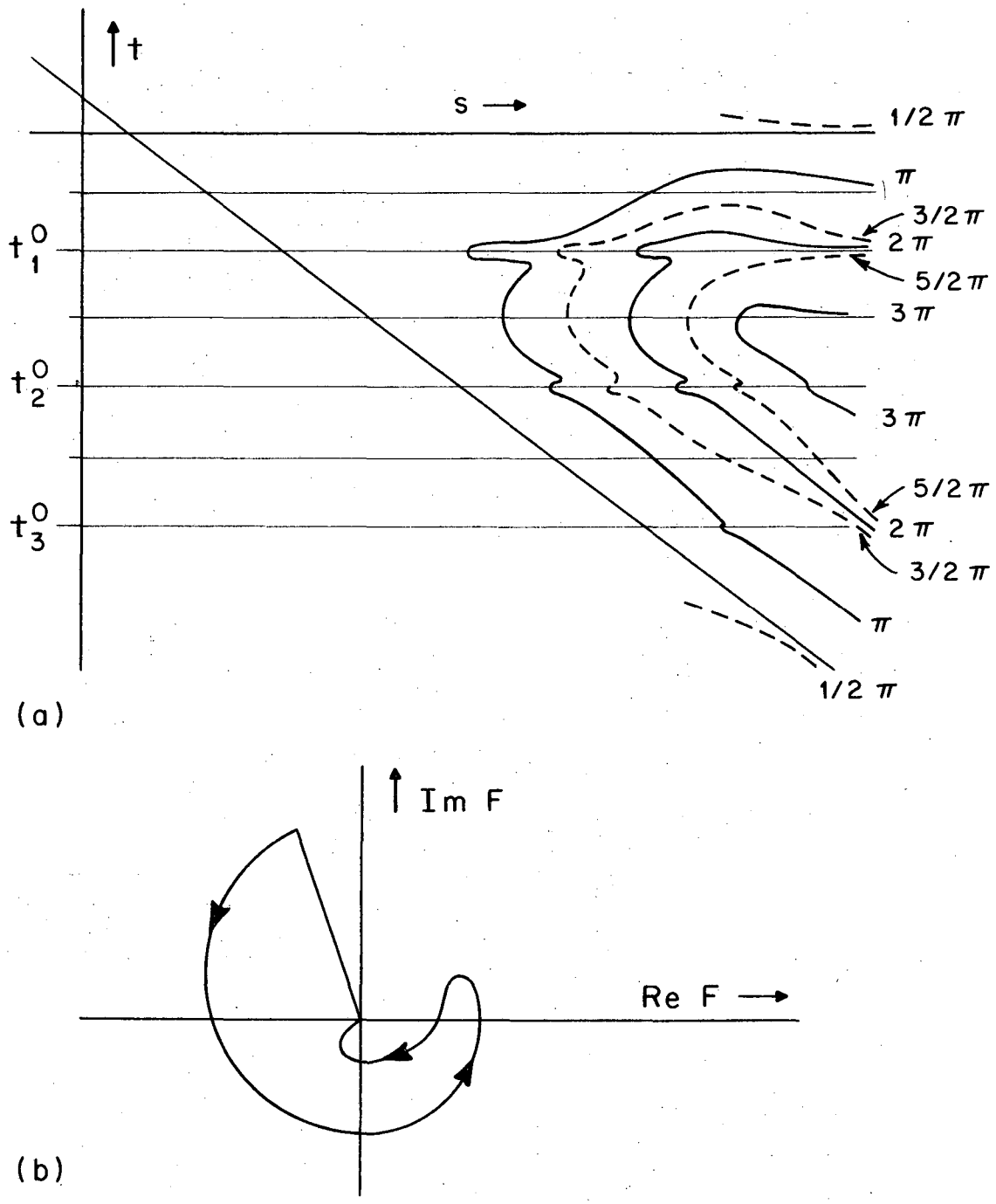

XBL6710-5473

Fig. 3.3

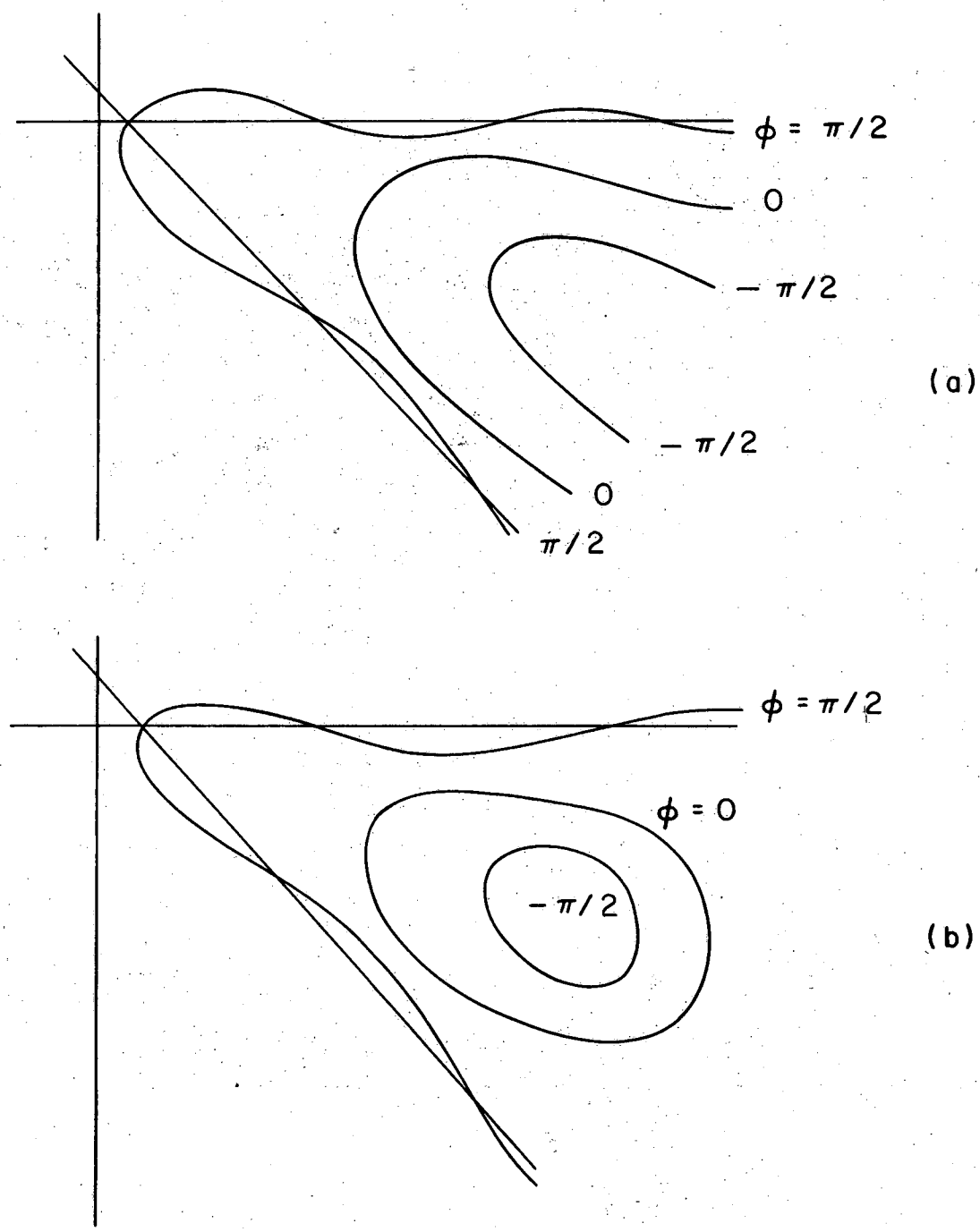

XBL6710-5474

Fig. 3.4

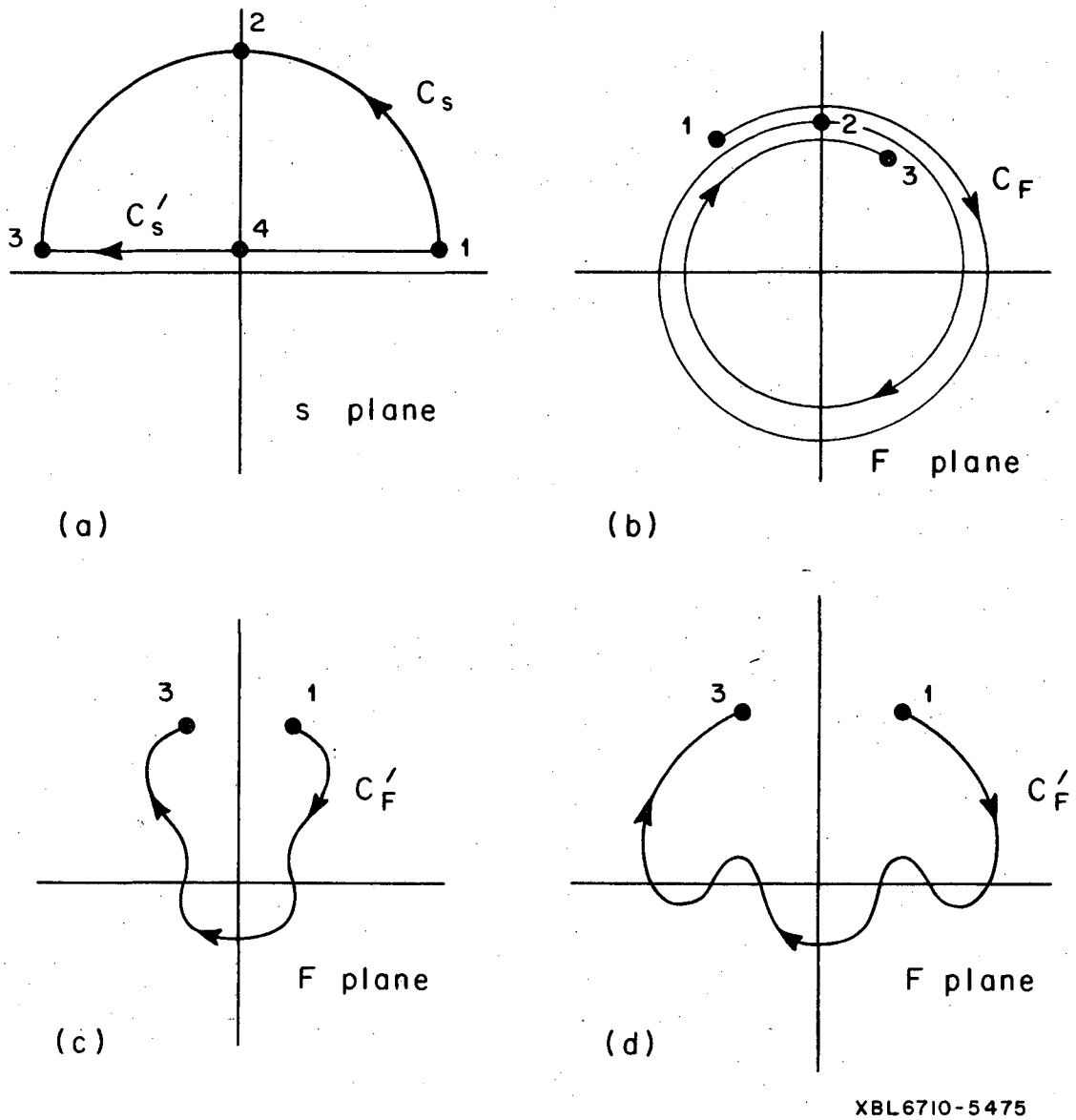
2
C_s
3
C_s'
4
1
s plane
(a)
1
2
3
C_F
F plane
(b)
3
1
C_F'
F plane
(c)
3
1
C_F'
F plane
(d)
XBL6710-5475

Fig. 4.1

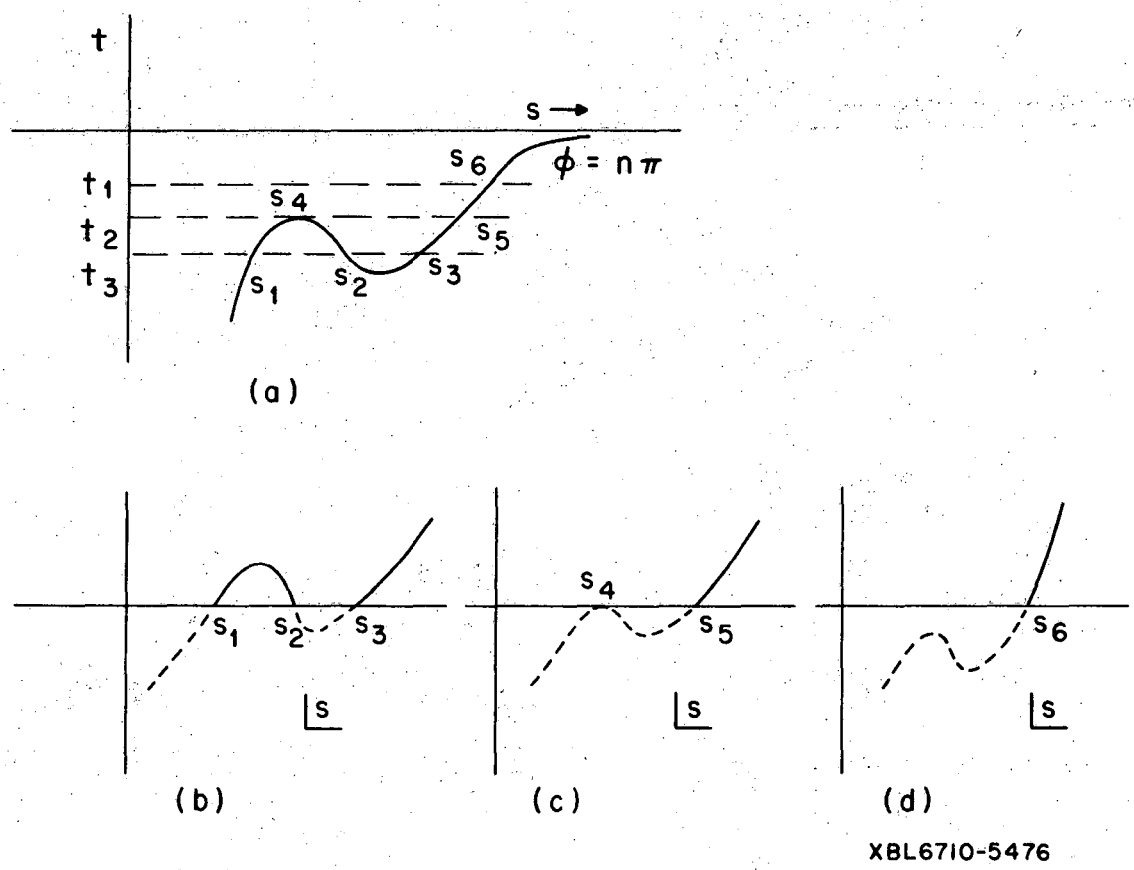
t
s →
t_1
t_2
t_3
s_1
s_2
s_3
s_4
s_5
s_6
$\phi = n\pi$
(a)
s_1
s_2
s_3
s
(b)
s_4
s_5
s
(c)
s_6
s
(d)
XBL6710-5476

Fig. 4.2

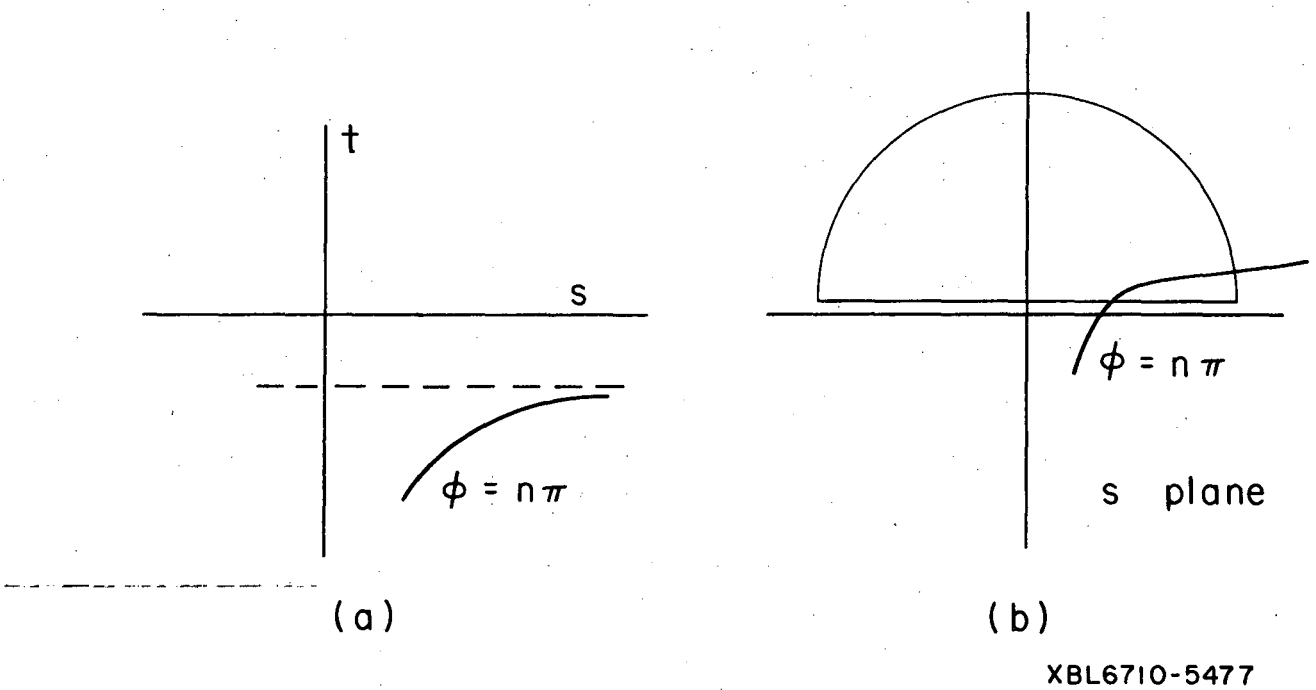

Fig. 4.3

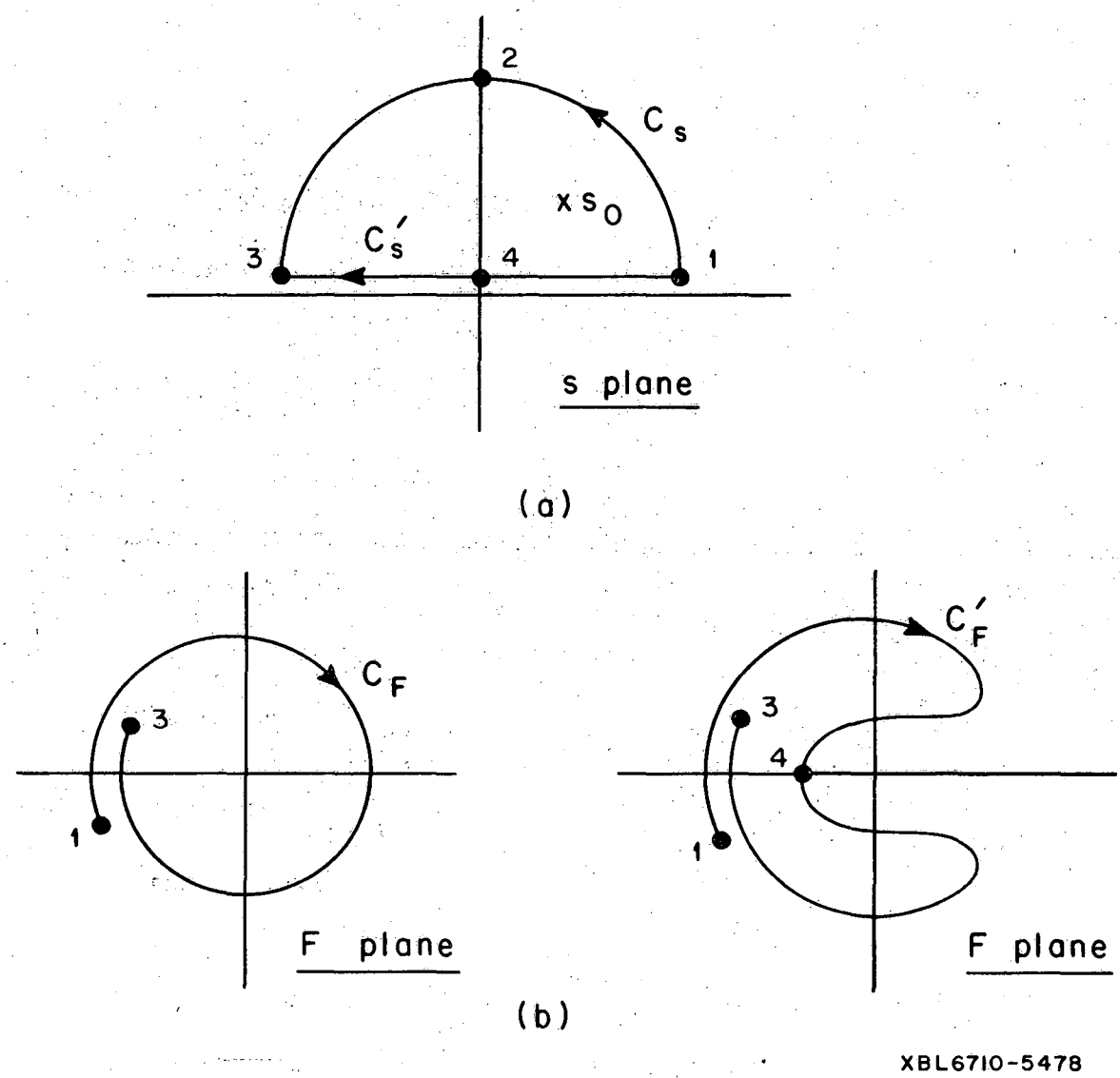
2
C_s
$x\,s_0$
3
C_s'
4
1
s plane
(a)
C_F
3
1
F plane
C_F'
3
4
1
F plane
(b)
XBL6710-5478

Fig. 4.4

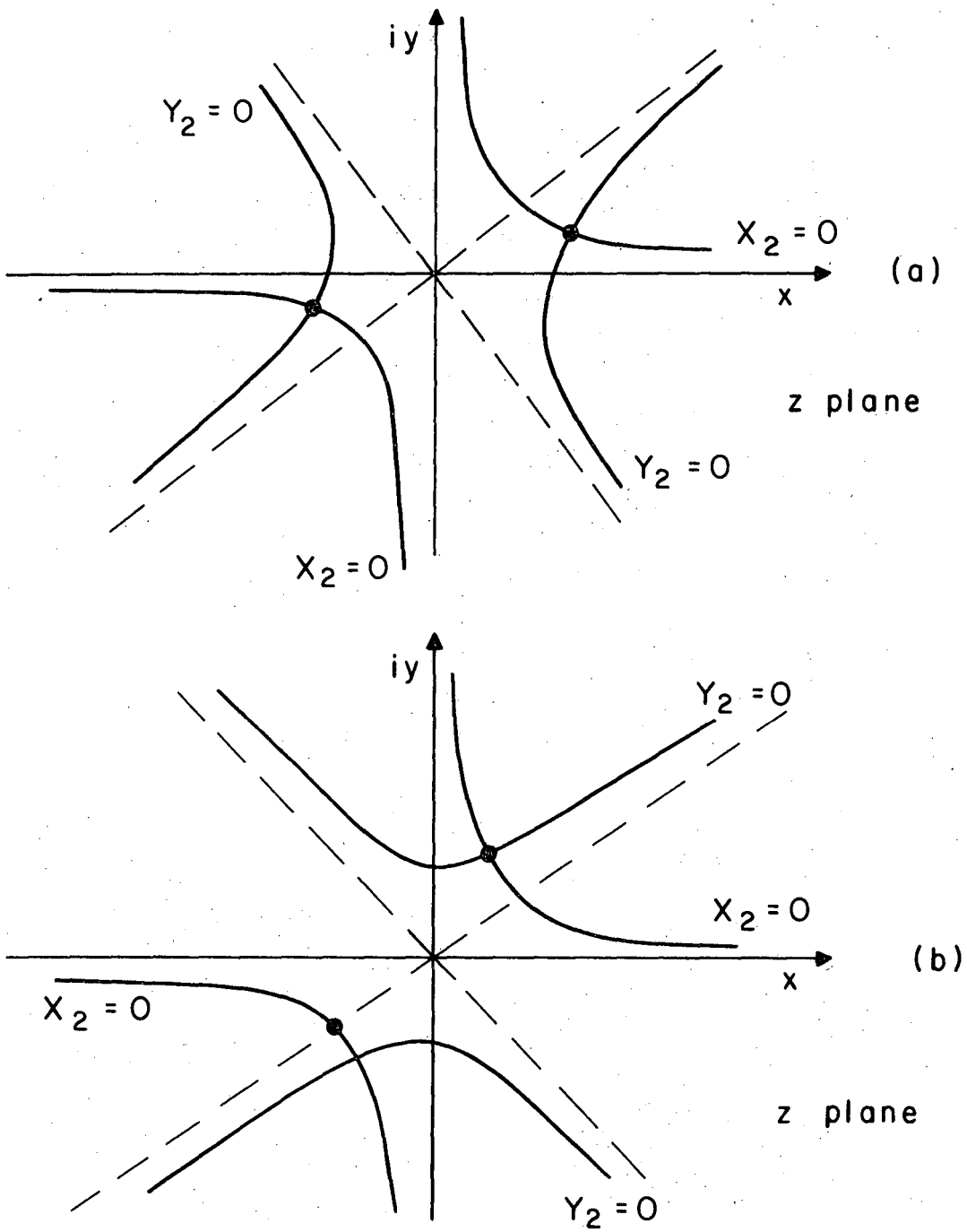
iy
$Y_2 = 0$
$X_2 = 0$
(a)
x
z plane
$Y_2 = 0$
$X_2 = 0$
iy
$Y_2 = 0$
$X_2 = 0$
(b)
x
$X_2 = 0$
z plane
$Y_2 = 0$
XBL6710-5479

Fig. 5.1

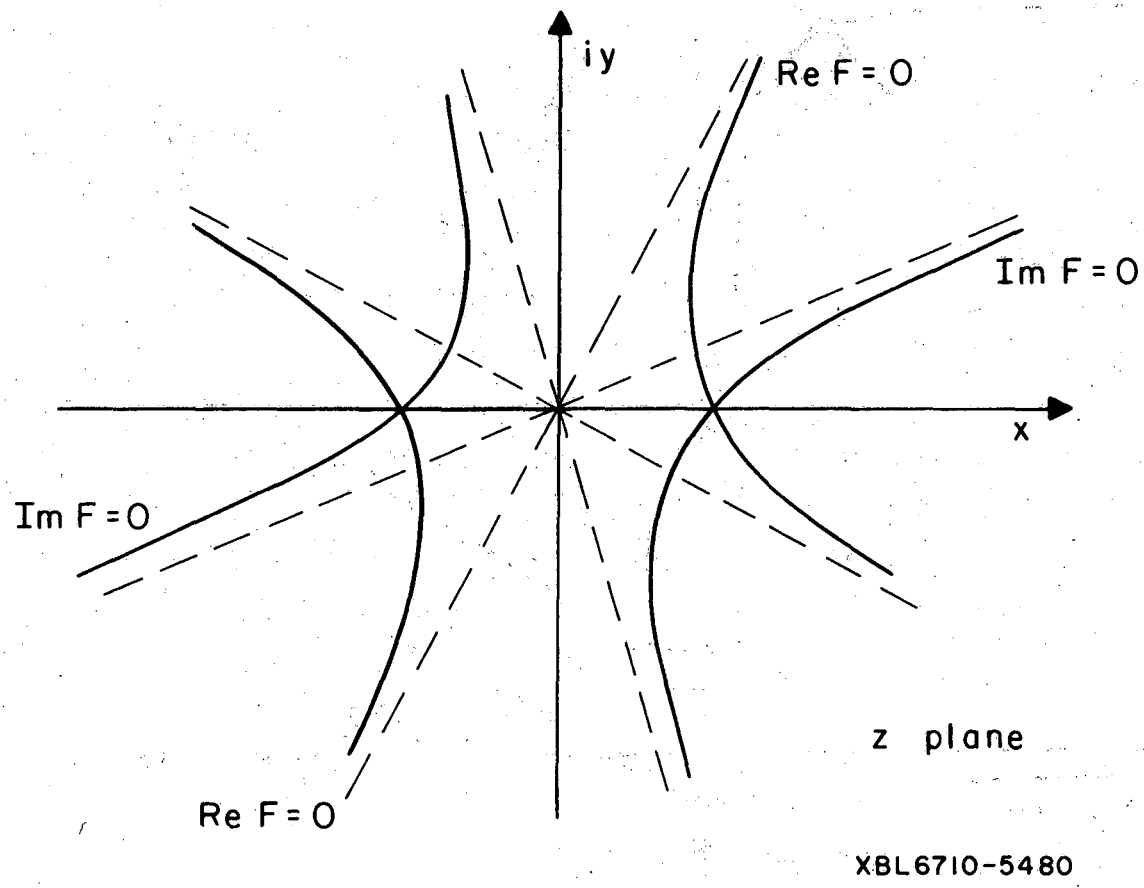

Fig. 5.2

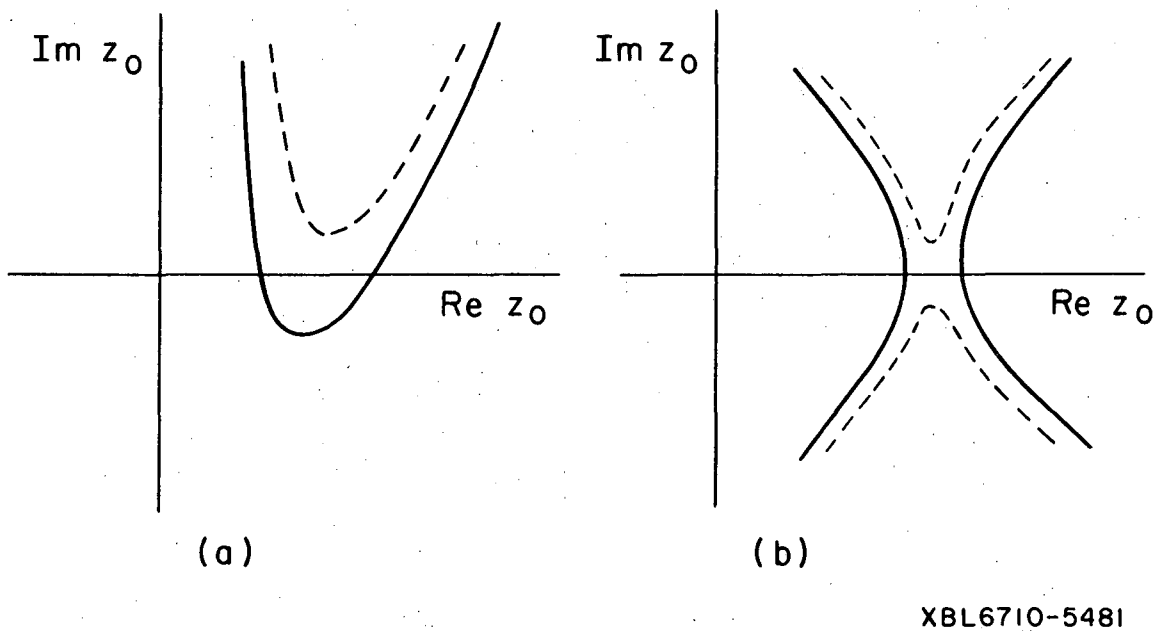

Fig. 5.3

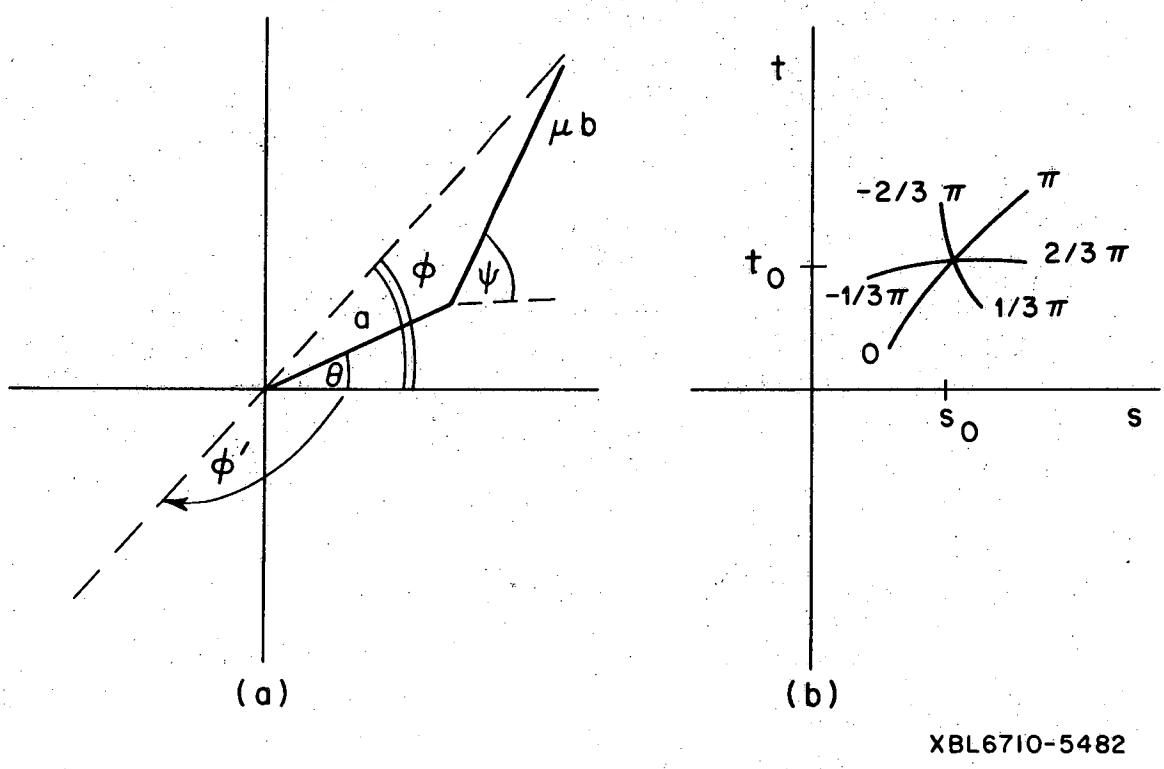

Fig. 5.4

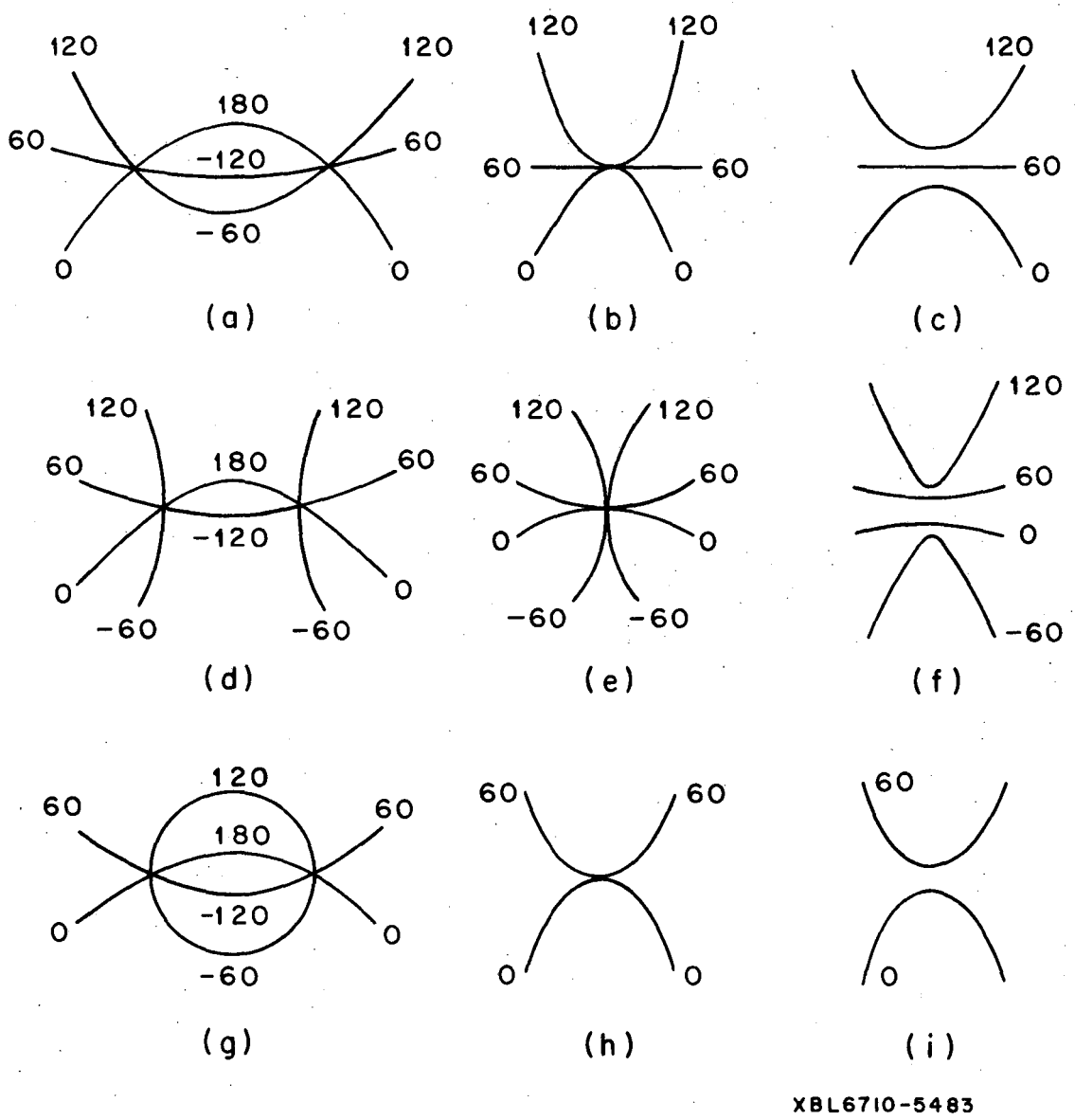

XBL6710-5483

Fig. 5.5

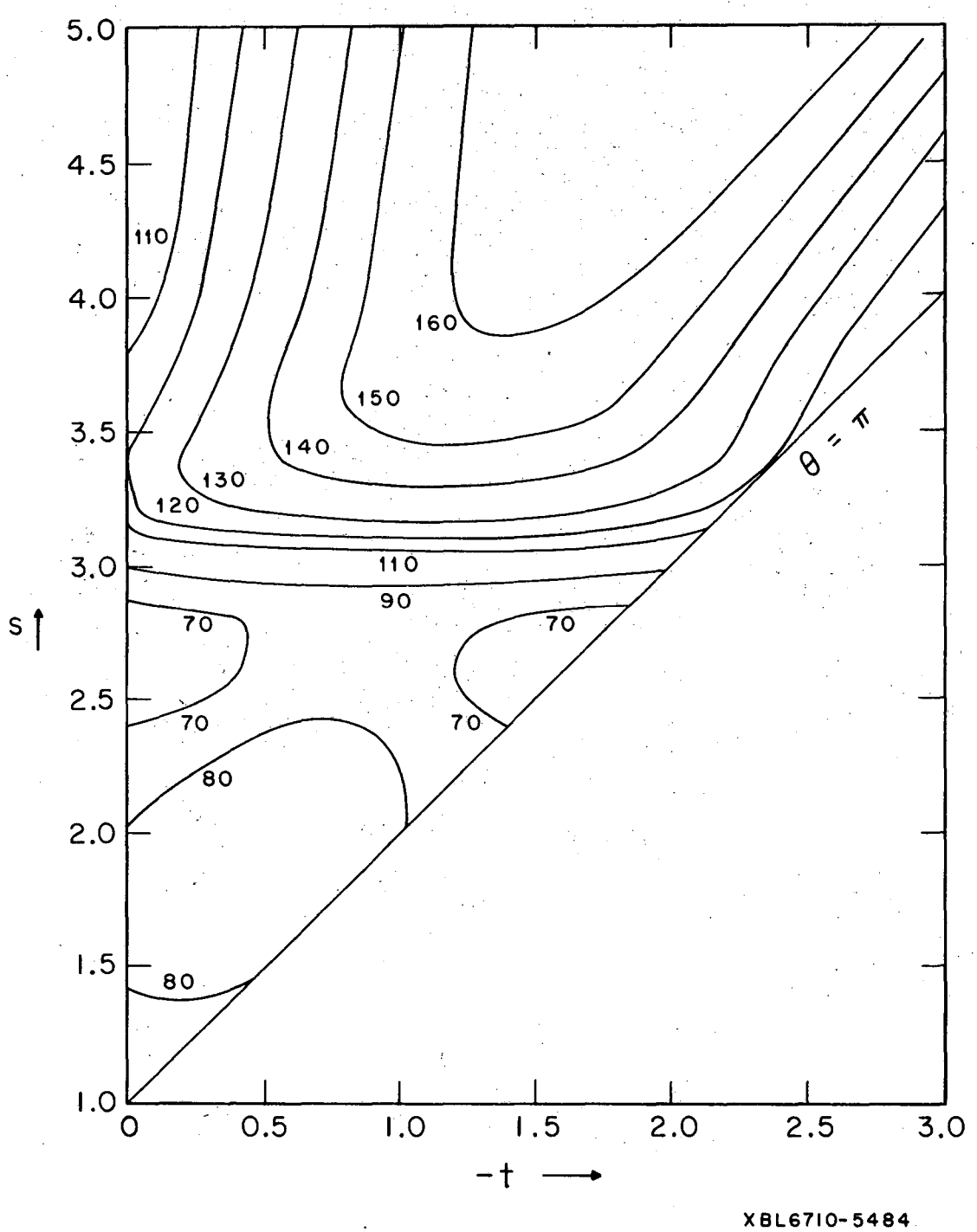
5.0
4.5
4.0
3.5
3.0
2.5
2.0
1.5
1.0
s
0
0.5
1.0
1.5
2.0
2.5
3.0
-t
110
160
150
140
130
120
110
90
70
70
70
70
80
80
θ = π
XBL6710-5484

Fig. 5.6

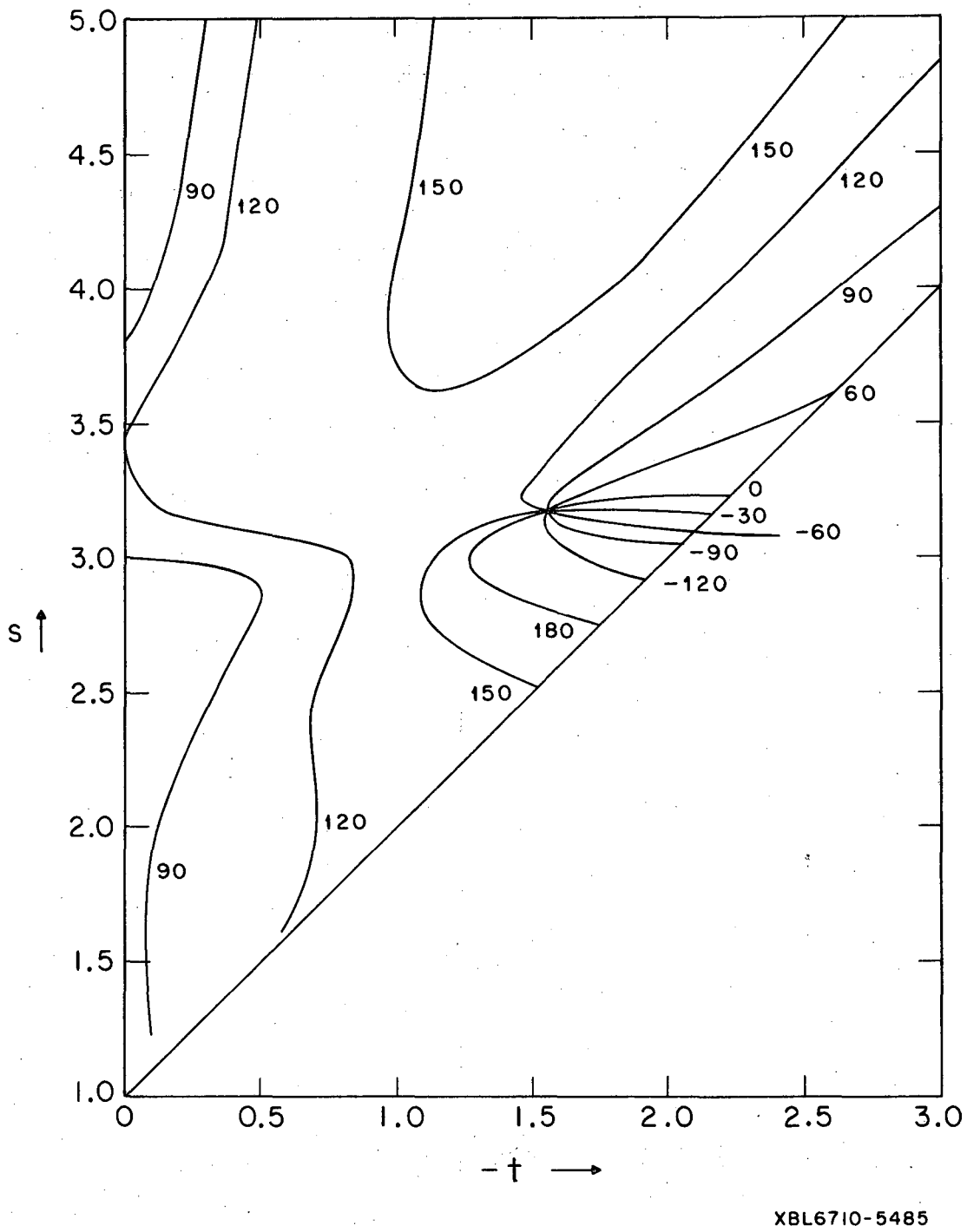
5.0
4.5
4.0
3.5
3.0
2.5
2.0
1.5
1.0
s
0
0.5
1.0
1.5
2.0
2.5
3.0
-t
90
120
150
150
120
90
60
0
-30
-60
-90
-120
180
150
120
90
XBL6710-5485

Fig. 5.7

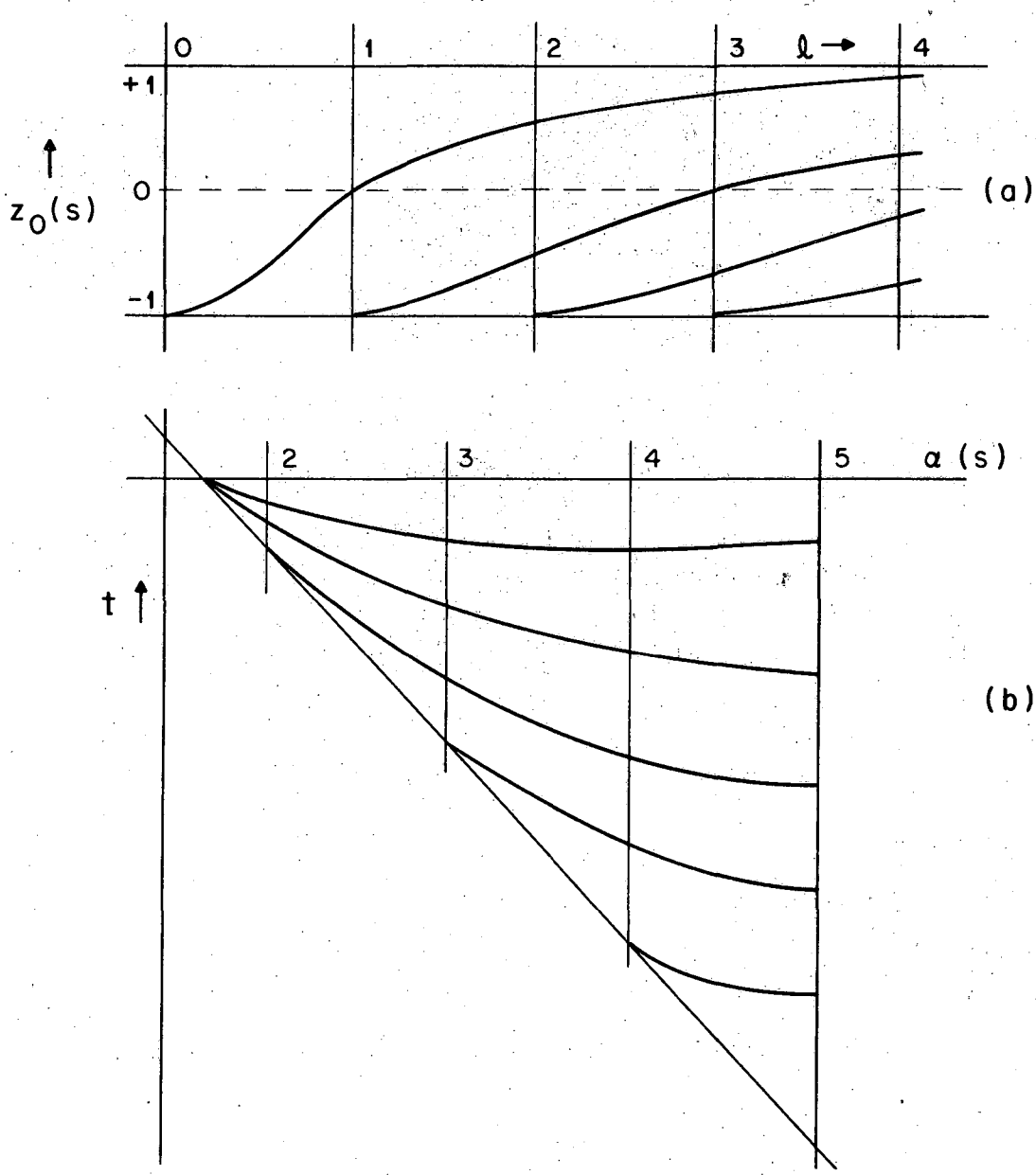

XBL6710-5486

Fig. 6.1

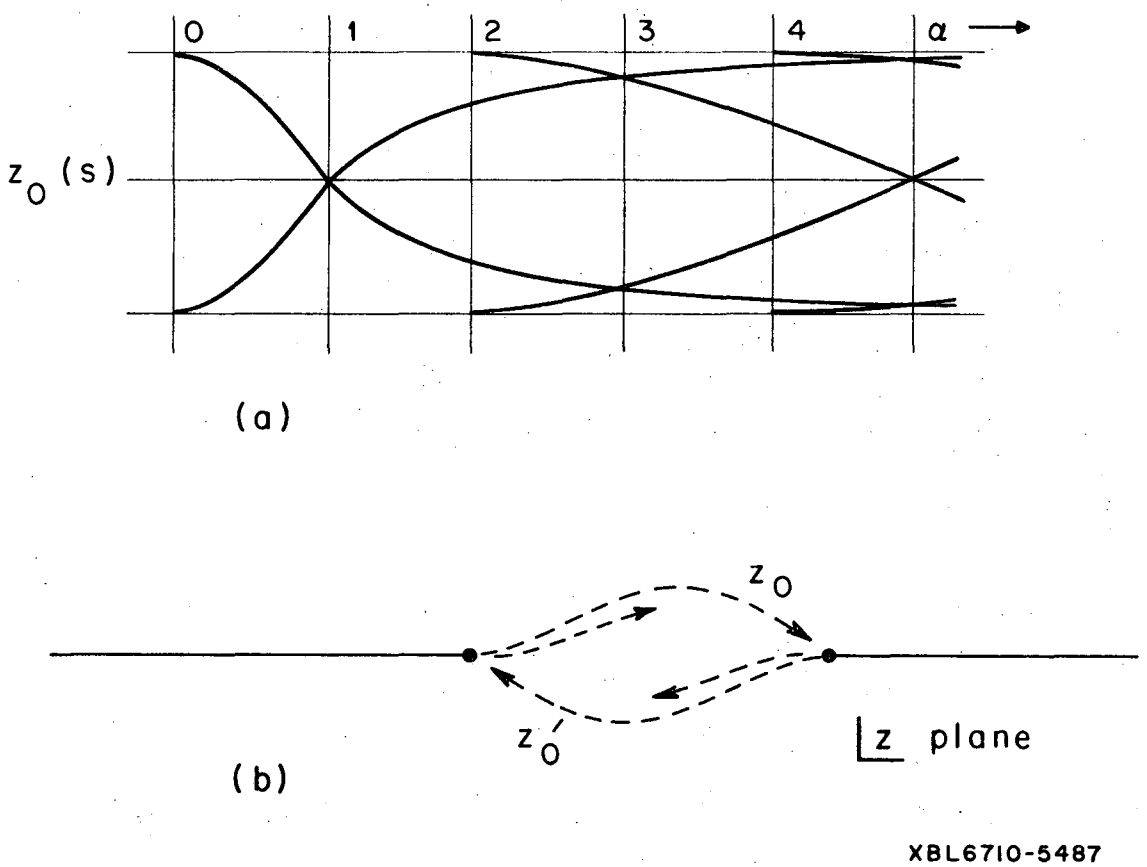

Fig. 6.2

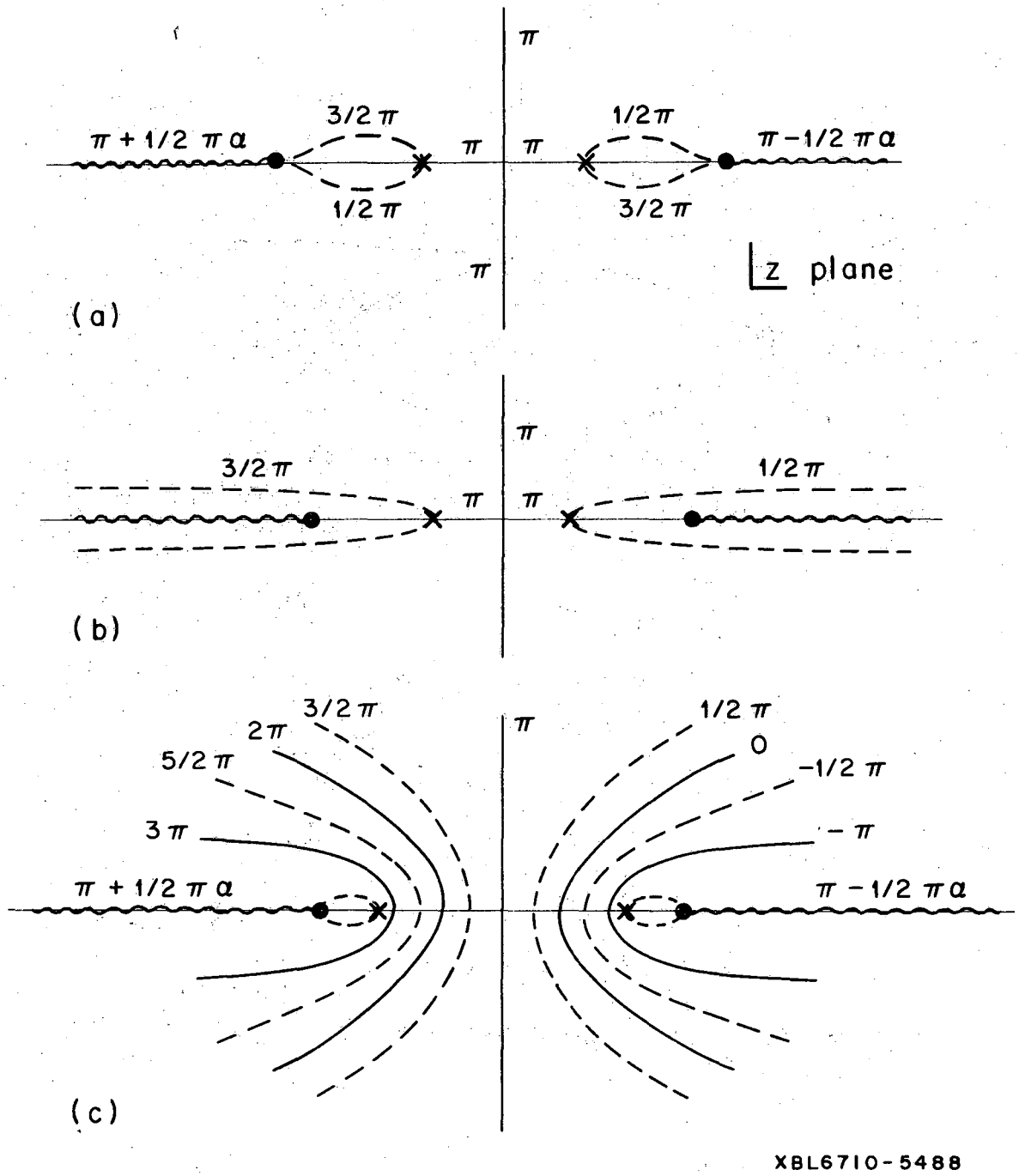
π
π + 1/2 π a
3/2 π
1/2 π
π
π
1/2 π
3/2 π
π − 1/2 π a
π
z plane
(a)
π
3/2 π
1/2 π
π
π
(b)
3/2 π
2 π
5/2 π
3 π
π + 1/2 π a
π
1/2 π
0
−1/2 π
− π
π − 1/2 π a
(c)
XBL6710-5488

Fig. 6.3

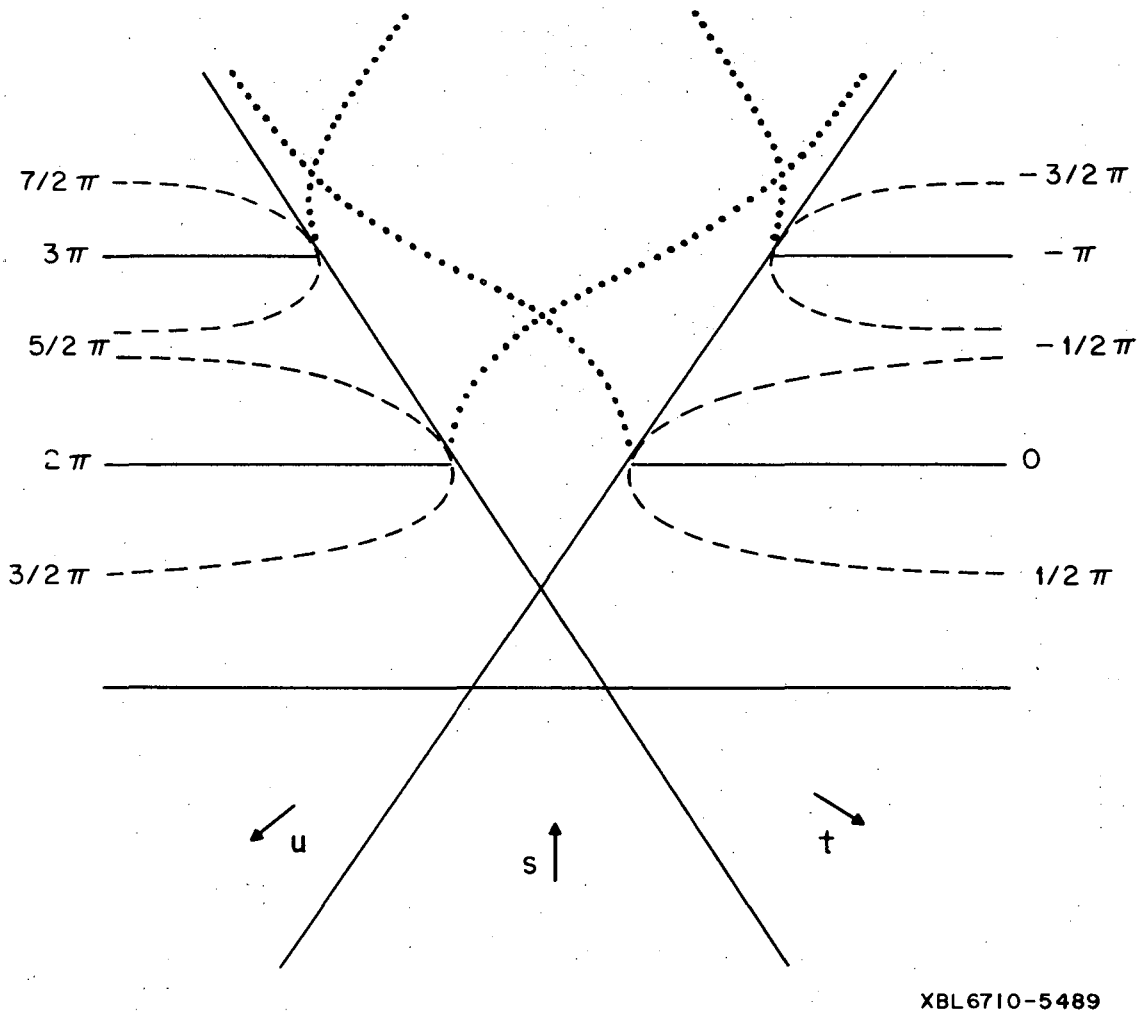

Fig. 6.4

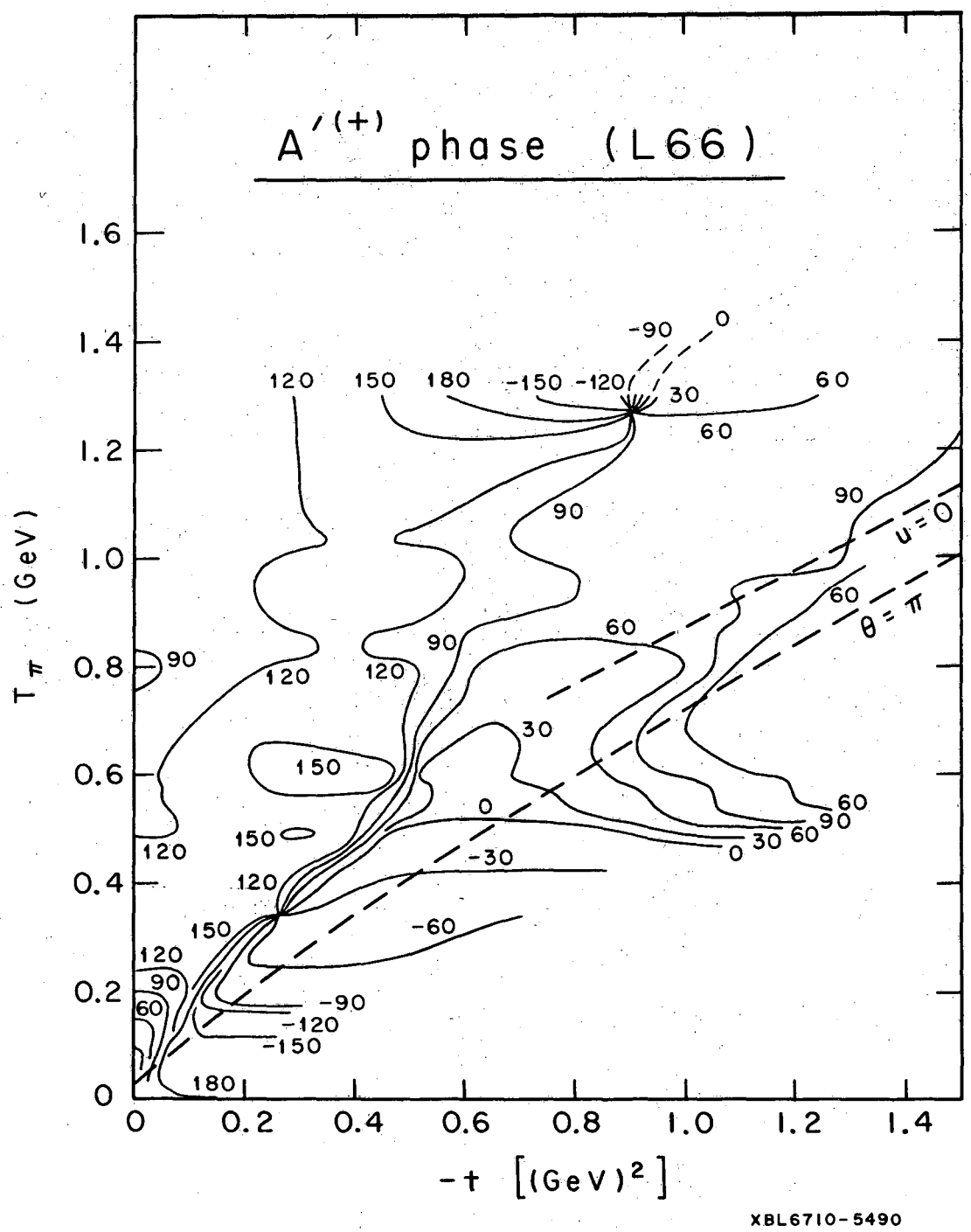

Fig. 7.1

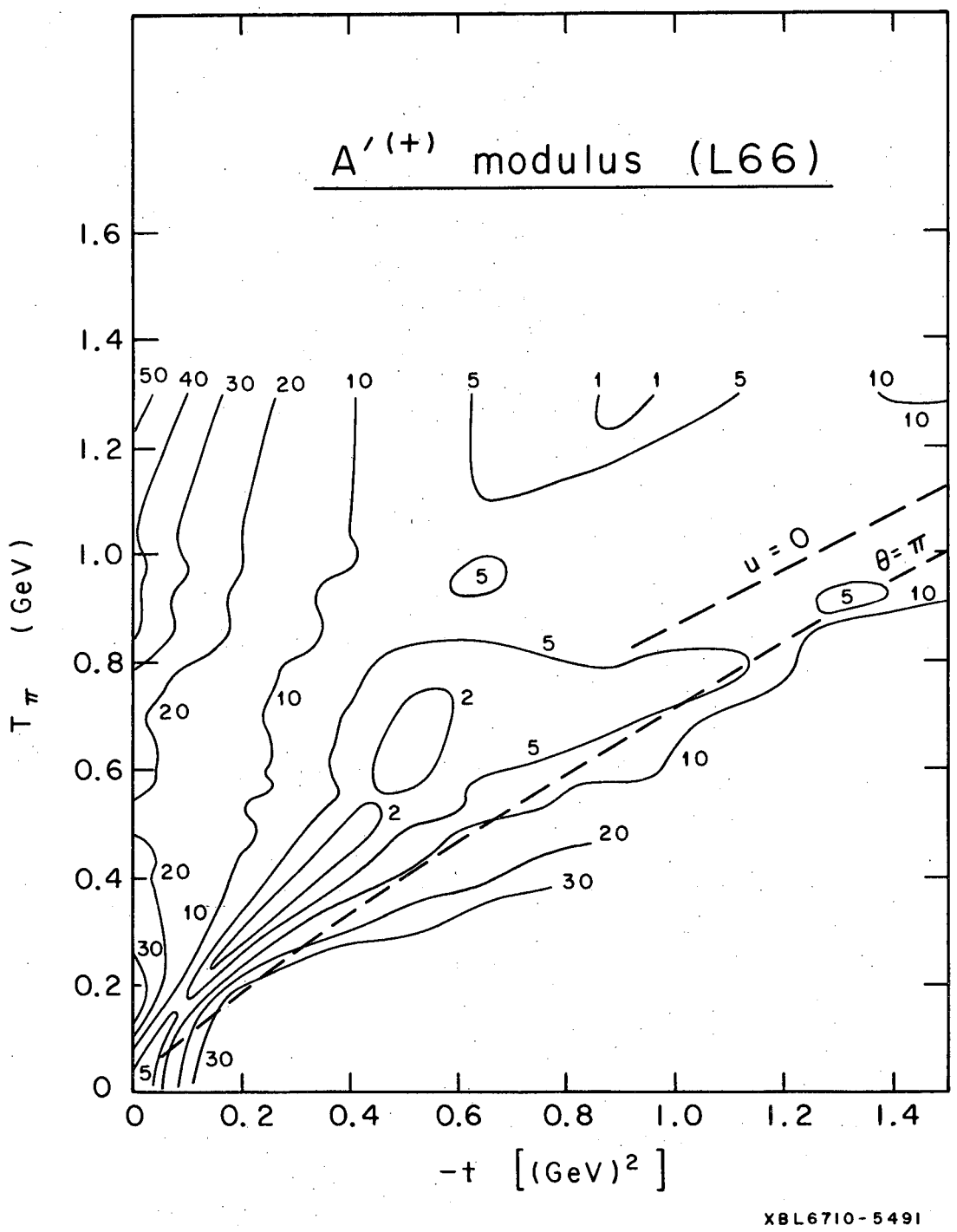

Fig. 7.2

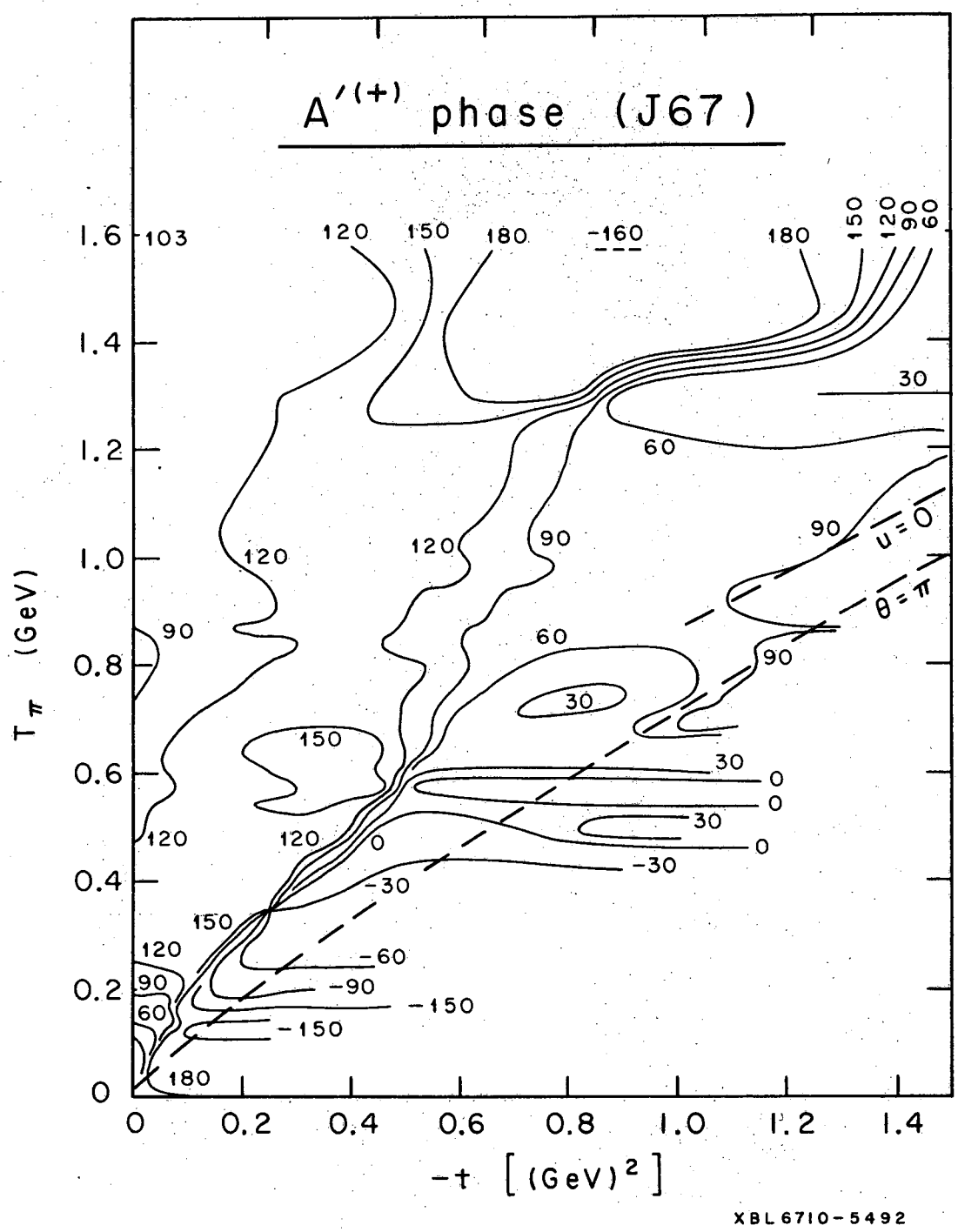

Fig. 7.3

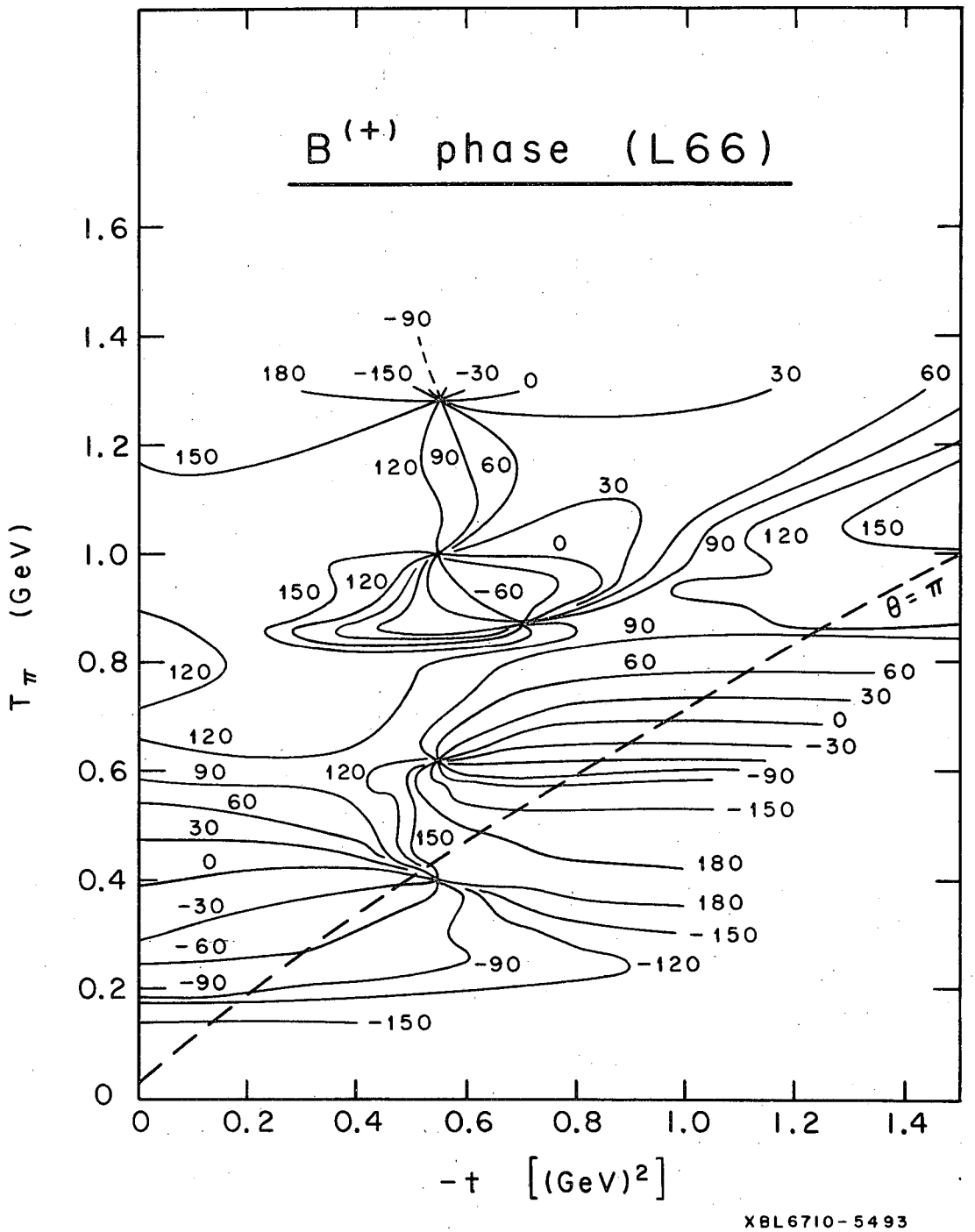

Fig. 7.4

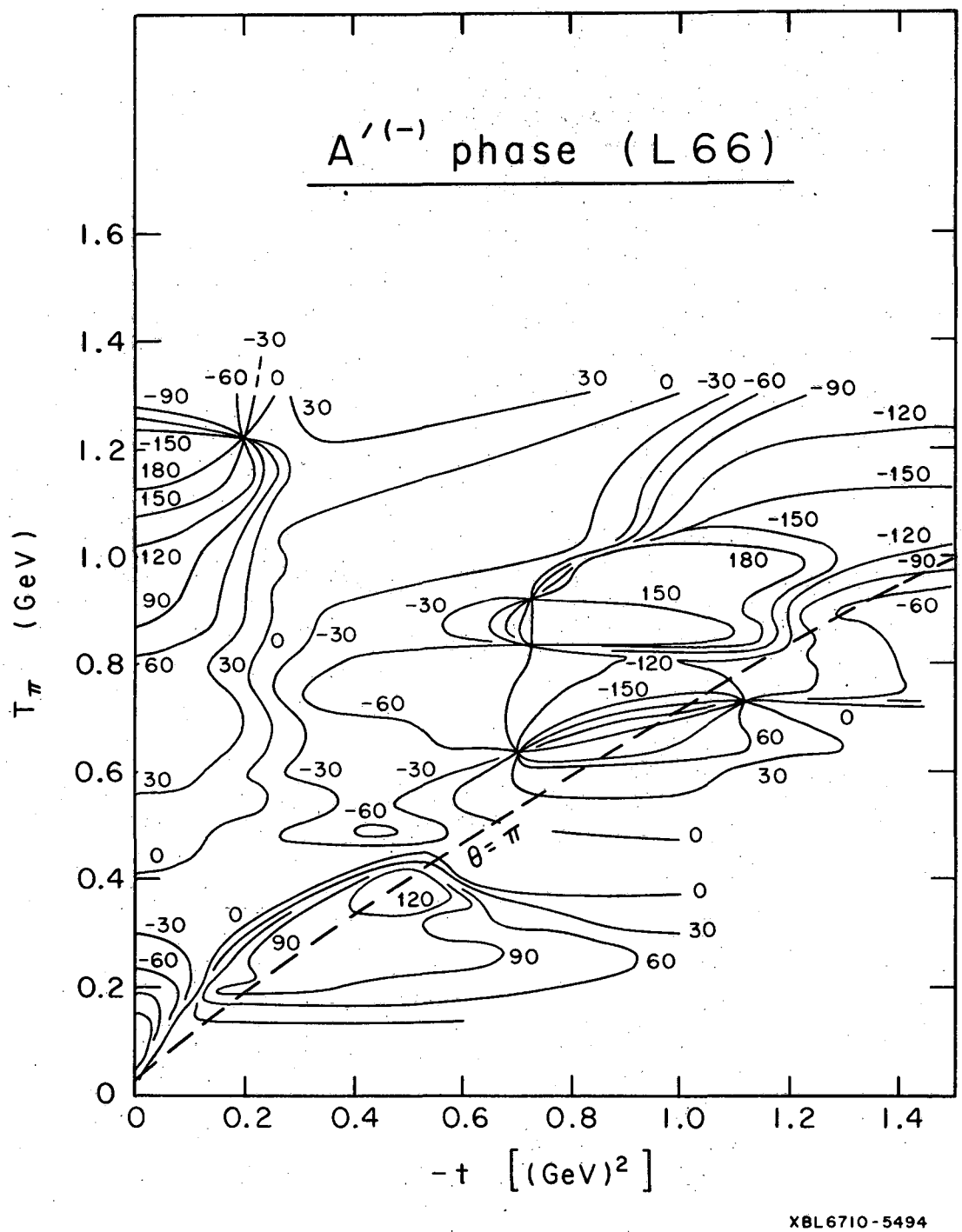

Fig. 7.5

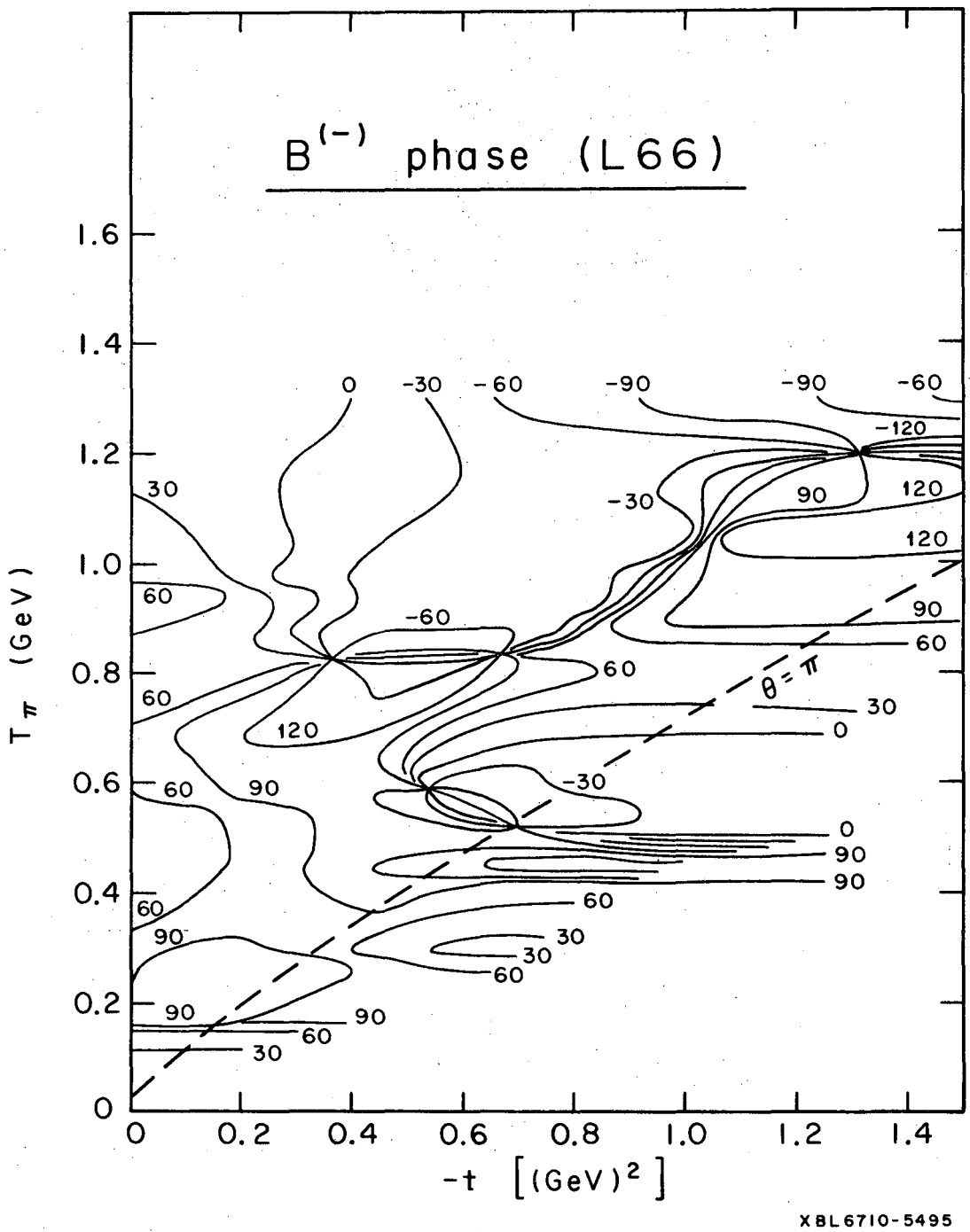

Fig. 7.6

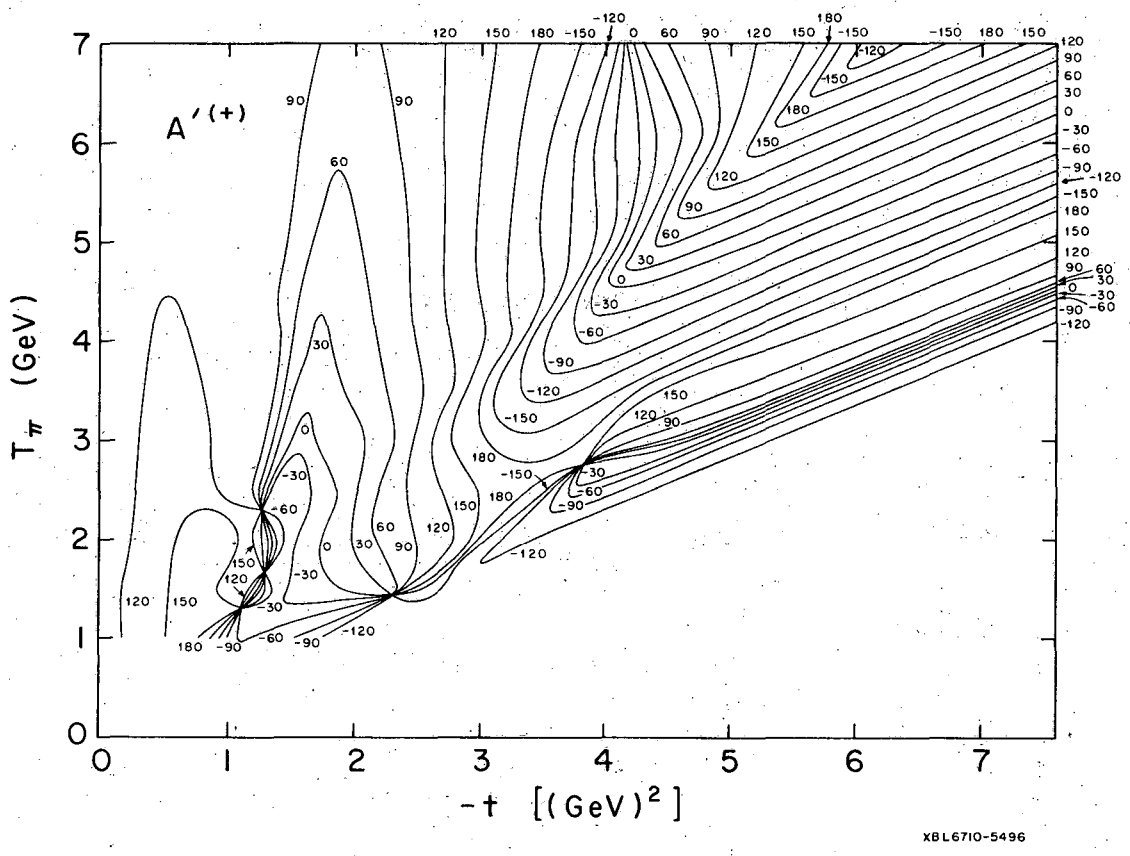

Fig. 8.1

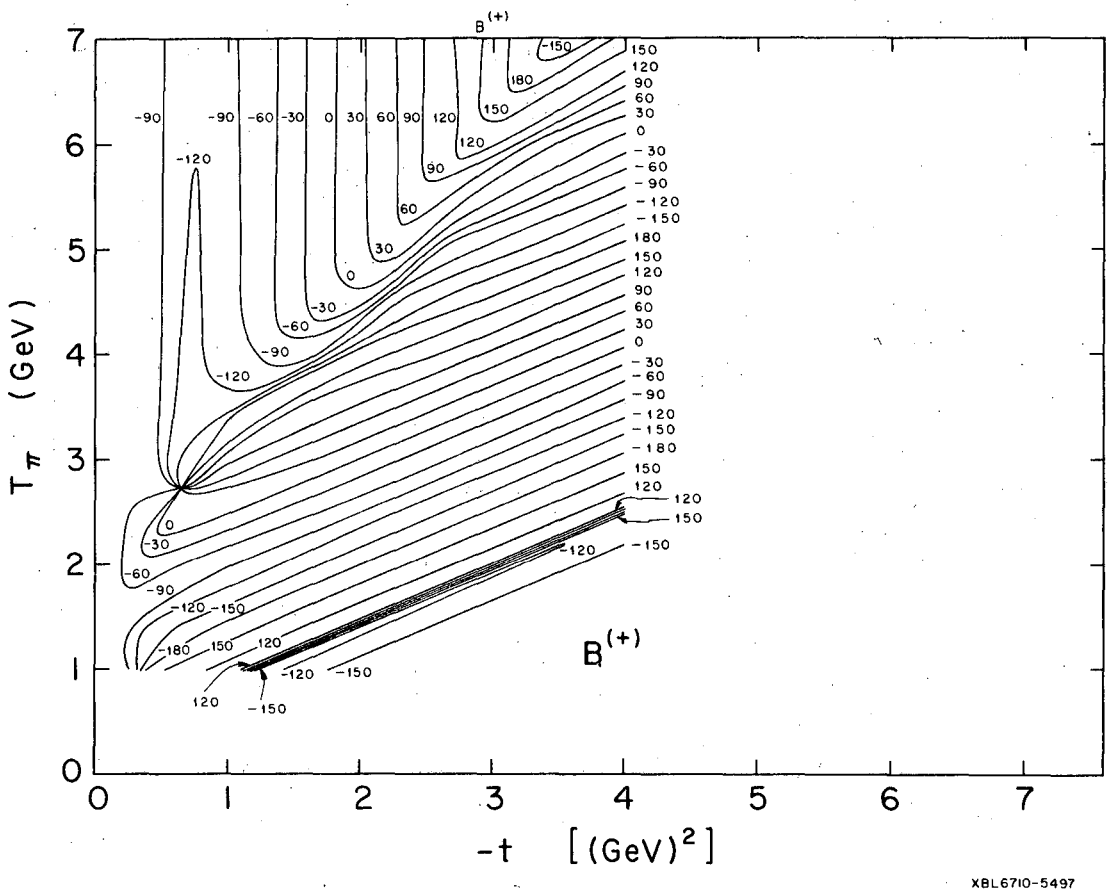

Fig. 8.2

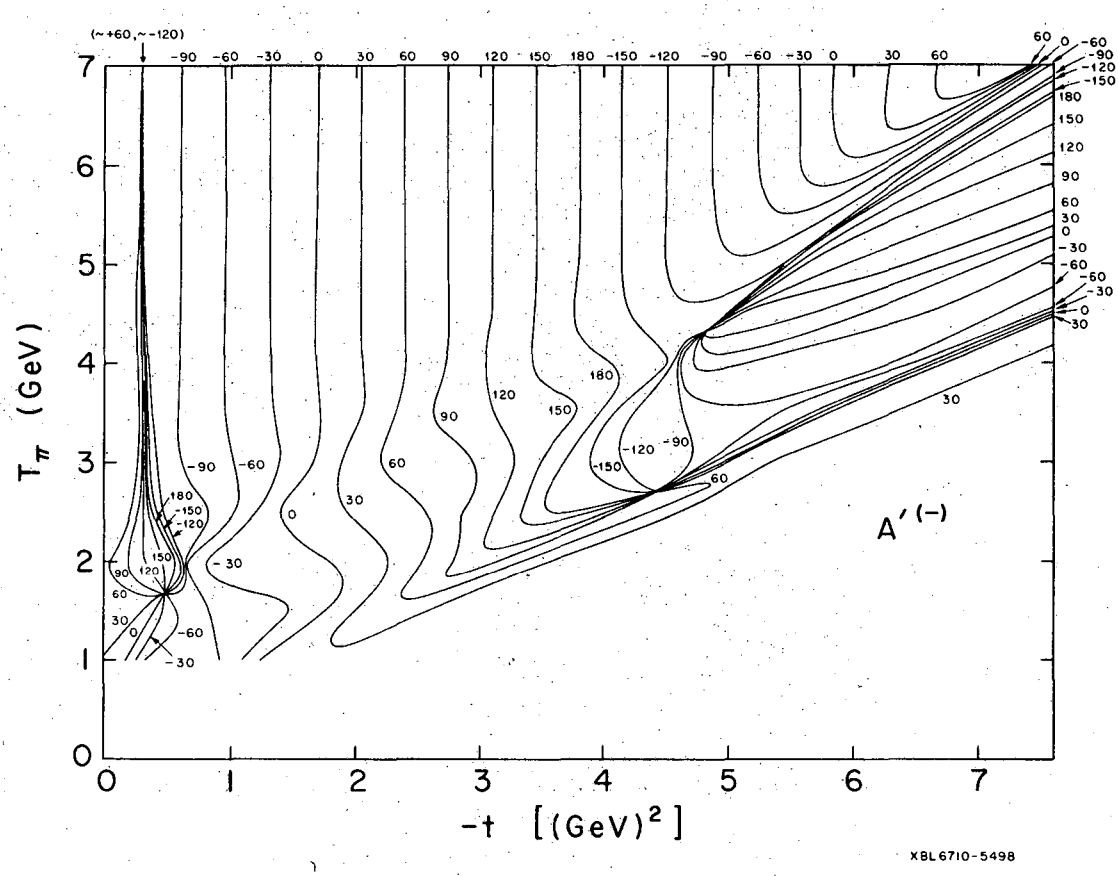

Fig. 8.3

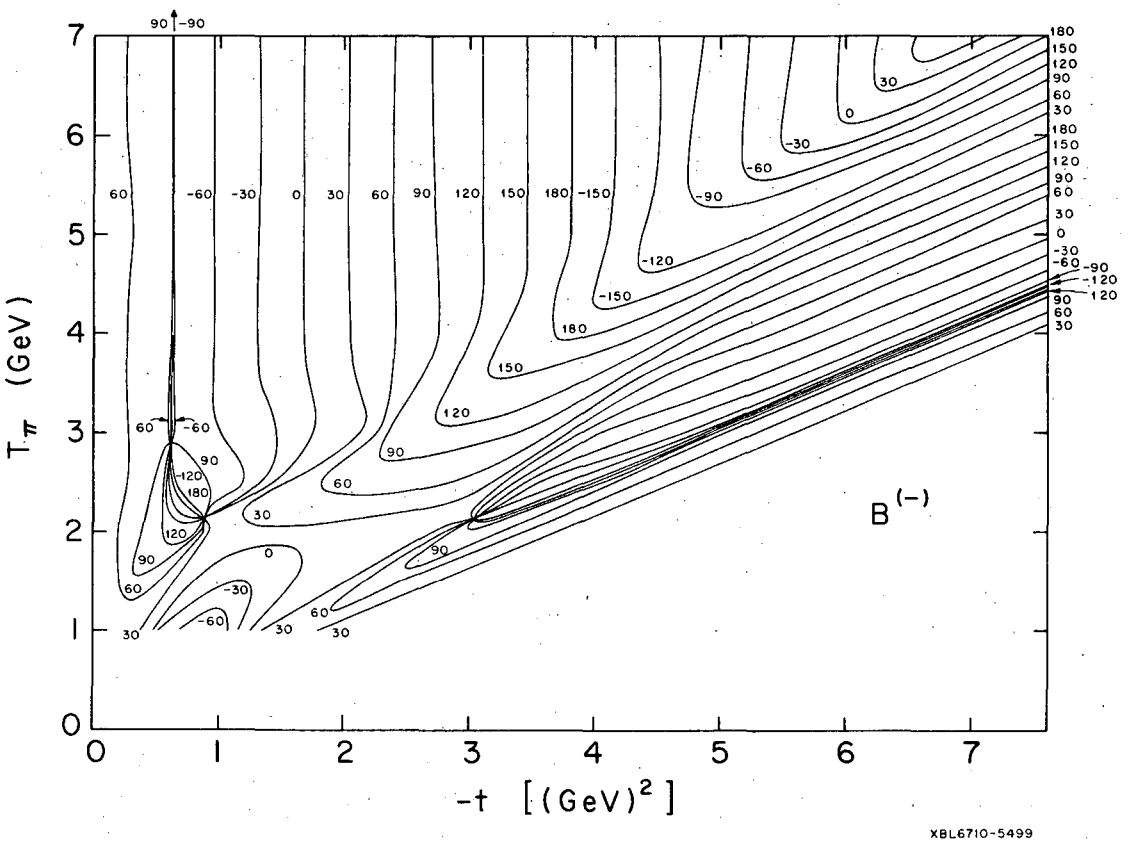

Fig. 8.4

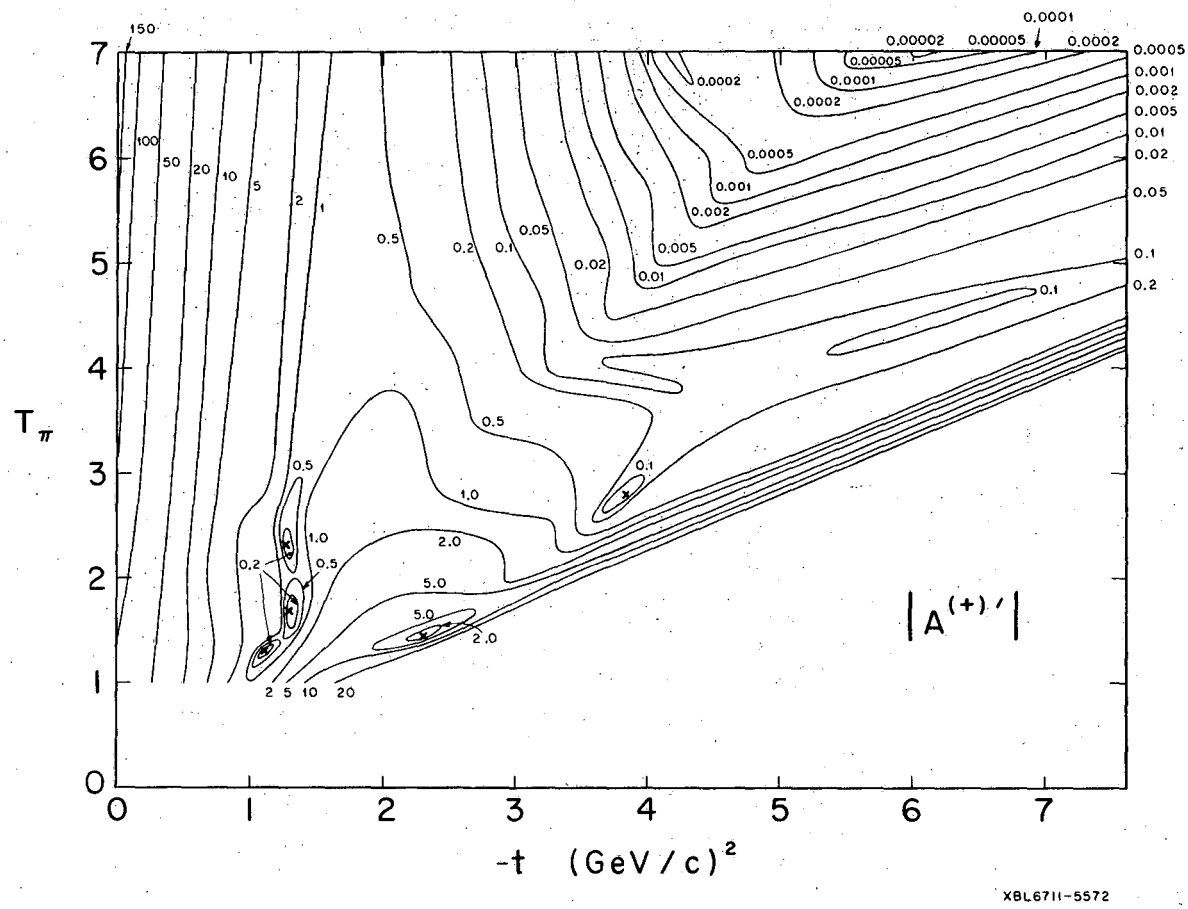

Fig. 8.5

This report was prepared as an account of Government sponsored work. Neither the United States, nor the Commission, nor any person acting on behalf of the Commission:

A. Makes any warranty or representation, expressed or implied, with respect to the accuracy, completeness, or usefulness of the information contained in this report, or that the use of any information, apparatus, method, or process disclosed in this report may not infringe privately owned rights; or

B. Assumes any liabilities with respect to the use of, or for damages resulting from the use of any information, apparatus, method, or process disclosed in this report.

As used in the above, "person acting on behalf of the Commission" includes any employee or contractor of the Commission, or employee of such contractor, to the extent that such employee or contractor of the Commission, or employee of such contractor prepares, disseminates, or provides access to, any information pursuant to his employment or contract with the Commission, or his employment with such contractor.